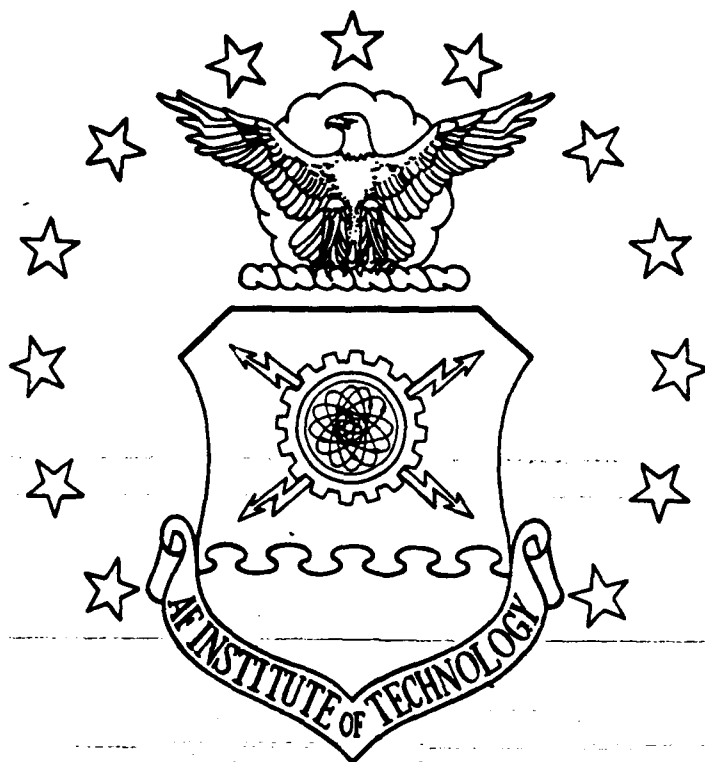




AD-A223 088



INTEGRATED STRUCTURAL/CONTROL DESIGN
VIA MULTIOBJECTIVE OPTIMIZATION

DISSERTATION

Garret L. Schneider
Captain, USAF

AFIT/DS/ENY/90-02

DISTRIBUTION STATEMENT A

Approved for public release;
Distribution Unlimited

DEPARTMENT OF THE AIR FORCE
AIR UNIVERSITY

AIR FORCE INSTITUTE OF TECHNOLOGY

Wright-Patterson Air Force Base, Ohio

90 06 20 058

DTIC
ELECTE
JUN 21 1990
S E D

AFIT/DS/ENY/90-02

INTEGRATED STRUCTURAL/CONTROL DESIGN
VIA MULTIOBJECTIVE OPTIMIZATION

DISSERTATION

Garret L. Schneider
Captain, USAF

AFIT/DS/ENY/90-02

DTIC
ELECTE
JUN 21 1990
S E D

Approved for public release; distribution unlimited

INTEGRATED STRUCTURAL/CONTROL DESIGN
VIA MULTIOBJECTIVE OPTIMIZATION

DISSERTATION

Presented to the Faculty of the School of Engineering
of the Air Force Institute of Technology
Air University
In Partial Fulfillment of the
Requirements for the Degree of
Doctor of Philosophy



Garret L. Schneider, B.S., M.S.
Captain, USAF

May 1990

| | |
|--------------------|--|
| Accession For | |
| NTIS GRA&I | <input checked="checked" type="checkbox"/> |
| DTIC TAB | <input checked="checked" type="checkbox"/> |
| Unannounced | <input type="checkbox"/> |
| Justification | |
| By _____ | |
| Distribution/ | |
| Availability Codes | |
| Dist | Avail and/or Special |
| A-1 | |

Approved for public release; distribution unlimited

INTEGRATED STRUCTURAL/CONTROL DESIGN
VIA MULTIOBJECTIVE OPTIMIZATION

Garret L. Schneider, B.S., M.S.
Captain, USAF

Approved:



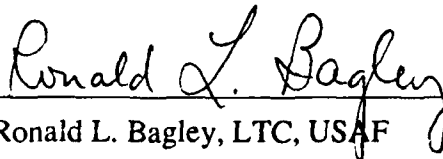
Robert A. Calico, Jr., Chairman

10 MAY 1990



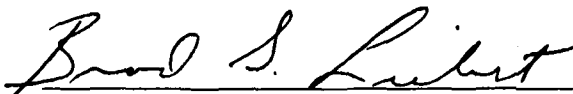
Vadim Komkov

10 MAY 1990



Ronald L. Bagley, LTC, USAF

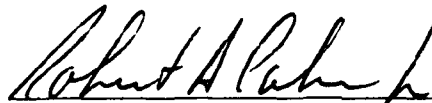
10 MAY 1990



Brad S. Liebst

10 MAY 1990

Accepted:



Robert A. Calico, Jr.
Interim Dean, School of Engineering

10 MAY 1990

Acknowledgments

It is with mixed emotions that I close this chapter of my life and move on with my career. I, of course, could not have finished this research without the help and guidance from many others. In particular, I thank my committee members, Dr Vadim Komkov and Lt Col Ronald Bagley, for their help and advice, as well as Dr Brad Liebst for his careful the thorough review of my work. But I owe particular thanks and gratitude to my research committee chairman and advisor, Dr Robert Calico, Jr. He guided me through all the ups and downs, kept me on track when things went astray, and was always willing and available to help whenever I needed it. I will miss working with these fine people.

My family has had to put up with the impact of my work on what could otherwise have been a normal family existence. I thank my wife, Susanne, for her help and understanding, and my boys Garret (Wulf) and Chase (Turk) for being there for me. I will always be there for them.

Garret L. Schneider

Table of Contents

| | Page |
|--|------|
| Acknowledgements | iii |
| List of Figures | vi |
| List of Tables | vii |
| List of Symbols | viii |
| Abstract | xii |
| I. Introduction | 1-1 |
| II. Background | 2-1 |
| Scalar Approach | 2-1 |
| Multiobjective Optimization | 2-2 |
| Pareto Optimality | 2-3 |
| Minimum Correction Homotopy Approach | 2-5 |
| III. Problem Formulation | 3-1 |
| IV. Model Description | 4-1 |
| Vibrational Motion | 4-2 |
| Kinetic Energy | 4-3 |
| Potential Energy | 4-8 |
| System Matrices | 4-9 |
| Model Order | 4-11 |
| Actuators and Sensors | 4-15 |
| V. Optimization Technique | 5-1 |
| Minimum Correction Homotopy Algorithm | 5-1 |
| Vector Objective Function | 5-4 |
| Derivatives | 5-4 |
| Design Procedure | 5-10 |
| VI. Integrated Structural/Control Optimal Design Results | 6-1 |
| Eigenvalue Placement | 6-2 |
| Mass Reduction | 6-3 |
| Control Effort Reduction | 6-3 |
| Mass and Control Effort Reduction | 6-5 |
| Spillover Sensitivity | 6-6 |

| | Page |
|---|--------|
| VII. Spillover Control | 7-1 |
| Constrained Solutions | 7-1 |
| Modal Suppression | 7-4 |
| Technique | 7-4 |
| Results | 7-6 |
| VIII. Conclusions | 8-1 |
| IX. Recommendations | 9-1 |
| Appendix A : Final Design Vector Values | A-1 |
| Appendix B : Final Design Gains | B-1 |
| Appendix C : Weighting Matrices | C-1 |
| Bibliography | BIB-1 |
| Vita | VITA-1 |

List of Figures

| Figure | Page |
|---|------|
| 4-1. The Draper/RPL configuration | 4-1 |
| 4-2. Draper/RPL configuration with reference frame and deflections defined | 4-2 |
| 4-3. Anti-symmetric deformation | 4-6 |
| 4-4. First five normal modes | 4-12 |
| 6-1. Case 1 eigenvalue trajectories | 6-4 |
| 6-2. Case 2 eigenvalue trajectories | 6-4 |
| 6-3. Damping ratio spillover sensitivity, design 1-Base (Case 1, baseline) | 6-7 |
| 6-4. Damping ratio spillover sensitivity, design 1-M50 (Case 1, 50% mass reduction) | 6-7 |
| 6-5. Damping ratio spillover sensitivity, design 1-CE50 (Case 1, 50% control effort reduction) | 6-8 |
| 6-6. Damping ratio spillover sensitivity, design 1-MCE50 (Case 1, 50% mass and control effort reduction) | 6-8 |
| 6-7. Damping ratio spillover sensitivity, design 2-MCE50 (Case 2, 50% mass and control effort reduction) | 6-9 |
| 7-1. Damping ratio spillover sensitivity with simple constraint spillover control, design 1-Base (Case 1, baseline) | 7-3 |
| 7-2. Damping ratio spillover sensitivity with simple constraint spillover control, design 1-MCE50 (Case 1, 50% mass and control effort reduction) | 7-3 |

List of Tables

| Table | Page |
|---|------|
| 4-1. Frequencies for first nine normal modes | 4-13 |
| 4-2. Draper/RPL configuration parameters | 4-14 |
| 5-1. MCH procedure | 5-3 |
| 6-1. Control efforts for reduced-mass designs | 6-5 |
| 7-1. Damping ratios with modal suppression, design 1-Base (Case 1, baseline) | 7-8 |
| 7-2. Damping ratios with modal suppression, design 1-MCE50 (Case 1, 50% mass and control effort reduction) | 7-9 |
| 7-3. Damping ratios with modal suppression, design 2-MCE50 (Case 2, 50% mass and control effort reduction) | 7-10 |

List of Symbols

| | | |
|-----------------|---|---|
| a | - | number of controls |
| \underline{b} | - | body-fixed reference frame unit vectors |
| \underline{c} | - | inequality constraint functions |
| d | - | number of design variables |
| \underline{e} | - | right closed-loop eigenvector |
| \underline{f} | - | left closed-loop eigenvector |
| \underline{h} | - | equality constraint functions |
| j | - | imaginary number (square root of -1) |
| m | - | mass |
| n | - | number of states |
| p | - | number of design objectives |
| \underline{r} | - | position vector |
| s | - | number of sensors |
| t | - | time |
| u | - | transverse body-fixed deformation, arms 1 and 2 |
| \underline{u} | - | vector of control inputs |
| v | - | transverse body-fixed deformation, arms 3 and 4 |
| \underline{w} | - | vector of generalized coordinates |
| \underline{x} | - | first-order state vector |
| \underline{y} | - | output vector |
| \underline{z} | - | vector of design variables |
| A | - | first-order state-space system matrix |
| A_{cl} | - | first-order state-space closed-loop system matrix |
| B | - | control influence matrix |

| | | |
|------------|---|--|
| C | - | symmetric positive semidefinite damping matrix |
| D | - | first-order state-space control influence matrix |
| E | - | right closed-loop eigenvector matrix |
| E_y | - | modulus of elasticity (Young's modulus) |
| F | - | left closed-loop eigenvector matrix |
| G | - | gain matrix |
| G_{uu} | - | control effort matrix |
| H | - | sensor influence matrix |
| I | - | identity matrix |
| I_a | - | arm area moment of inertia |
| I_h | - | hub moment of inertia |
| I_t | - | tip mass rotational moment of inertia |
| I_1 | - | arm 1 moment of inertia |
| I_3 | - | arm 3 moment of inertia |
| K | - | symmetric positive semidefinite stiffness matrix |
| L | - | arm length |
| L_g | - | Lagrangian |
| M | - | symmetric positive definite mass matrix |
| N_{sf} | - | number of admissible (shape) functions |
| P | - | potential energy |
| R | - | hub radius |
| T | - | kinetic energy |
| U | - | generalized displacement coordinates, arms 1 and 2 |
| V | - | generalized displacement coordinates, arms 3 and 4 |
| α | - | mass-proportional damping constant |
| α_H | - | homotopy parameter |

| | | |
|-----------------|---|--|
| β | - | stiffness-proportional damping constant |
| δ | - | partial derivative |
| δ_{ij} | - | Kronecker delta |
| Φ | - | open-loop eigenvector |
| γ | - | design objective |
| η | - | vector of modal coordinates |
| κ | - | arm height |
| λ | - | closed-loop eigenvalue |
| μ | - | comparison function |
| π | - | arm mass |
| θ | - | rigid-body rotation angle of body-fixed reference frame with respect to inertial reference frame |
| ρ | - | distance along arm |
| ρ_d | - | arm mass density |
| τ | - | arm thickness |
| u | - | control effort |
| ω | - | damped frequency |
| ξ | - | open-loop damping ratio |
| ψ | - | open-loop modal frequency |
| ζ | - | closed-loop damping ratio |
| Φ | - | system modal matrix |
| Γ | - | spillover annihilation matrix |
| Λ | - | diagonal matrix of closed-loop eigenvalues |
| Θ | - | attainable set |
| Ω | - | feasible set |
| \mathcal{R}^n | - | real n-dimensional space |

| | | |
|----------|---|-----------------|
| $[\]$ | - | diagonal matrix |
| \times | - | cross product |
| \cdot | - | dot product |

Subscripts

| | | |
|----|---|----------------|
| a | - | arm |
| cl | - | closed-loop |
| h | - | hub |
| p | - | position |
| s | - | sensor |
| sf | - | shape function |
| t | - | tip mass |
| u | - | control |
| v | - | velocity |
| 1 | - | arm 1 |
| 3 | - | arm 3 |

Superscripts

| | | |
|-------------|---|--|
| T | - | transpose |
| * | - | desired goal |
| (\cdot) | - | differentiation with respect to time [$d(\cdot)/dt$] |
| ' | - | spatial differentiation |

Abstract

A minimum correction homotopy approach is used to obtain the simultaneous/integrated optimal design of a large flexible structure and its active control system. Instead of the usual method of weighting and summing all desired objectives to form a constrained scalar optimization problem, a vector of objective functions is dealt with directly.

The Draper/RPL configuration (a central hub with four symmetric, identical arms) is the design structure. The design seeks to minimize the mass of the arms. Using simple feedback of arm displacements and velocities, the control system seeks to achieve specified closed-loop eigenvalues (frequencies and damping ratios) and control effort. Design variables are the arm dimensions, control system gains, and sensor and actuator locations. Not only can the structural design be accomplished while placing the closed-loop eigenvalues, but a simultaneous 50% reduction in mass and/or control effort can be obtained.

Since reduced-order models were used for the structural/control design, the resultant configurations are easily driven unstable by spillover from higher-order unmodeled modes. A modal suppression technique is applied to eliminate observation spillover and provide a decade of deadband above the controller bandwidth.

*Keywords: Control theory
control system analysis (KRL)*

INTEGRATED STRUCTURAL/CONTROL DESIGN VIA MULTIOBJECTIVE OPTIMIZATION

I. Introduction

The design of large flexible space structures presents distinct and often competing challenges to both structural dynamicists and control engineers. The need to maneuver such structures and then suppress resultant vibrations, or to reject disturbance vibrations from a variety of sources to meet exacting pointing and stability requirements is often directly opposed to the low stiffness and high flexibility accompanying a low weight design. Passive techniques to supplement structural damping justly receive much attention and are very important, but are not panaceas. The requirement for active control of large space structures is widely, if not universally, accepted.

Active control of large space structures has been extensively studied. Design methods have progressed well beyond the practice of adding active controls to make up for or 'fix' structural difficulties. However, design of actively controlled structures has traditionally been a sequential process: first the structure was designed based on structural criteria (minimize mass while achieving desired natural frequencies, mode shapes and dynamic response); then the control system was designed to meet desired closed-loop objectives (while minimizing controller work and the energy of the vibrating structure) for the given structural design. Inasmuch as a lower weight (higher flexibility) structure requires more control energy, the objectives of the two design steps are contradictory and an optimal controller placed on an optimally designed structure does not result in an optimal control-structure design.

A natural progression has been to incorporate the sequential approach into a design loop, repeating the process so that the design result improves with each iteration. However, the iterated design tends to be dominated by the first discipline in the sequence.

In the recent technical literature, the competitive natures of structural and active control system design are recognized. Attempts are made and interfaces are suggested to integrate the design process. However, because of the very strong, frequently unintentional and adverse coupling between the flexible structure and active control system, a wholistic or simultaneous approach to integrated structural/control design is necessary. In particular, a vector approach wherein both structural and control design objectives are treated in parallel will be developed.

Finally, it must be noted that designs are normally based on reduced-order models, especially of large flexible space structures, either due to considerations of on-board computer speed or the ability to accurately determine controller gains. Spillover from the higher-order (unmodeled) residual modes affects system performance and may well cause instability. Considerations of model order truncation effects must not be neglected in any structural/control design. An integrated design approach, as any other, is only as good as the information it is based upon.

This dissertation presents an approach to integrate structural and control design. First, previous work, using both scalar and multiobjective approaches, is reviewed (Chapter II). Next, the problem of an actively controlled structural system is formulated (Chapter III), followed by descriptions of how the structure and controller are modeled for this study (Chapter IV). In Chapter V the use of a minimum correction homotopy algorithm to optimize a vector objective function is discussed and applied to this integrated structural/control design problem. Chapter VI presents design results for various combinations of design objectives. An examination of the designs' sensitivity to spillover from higher-order modes leads to the two methods of spillover control and corresponding

results discussed in Chapter VII. Conclusions regarding this integrated design approach, including spillover control, and recommendations for future work are given in Chapters VIII and IX, respectively.

II. Background

Within the last several years, interest and research in integrated structural/control design has grown and been reported. Such design methods result in desired system response characteristics with lower mass and possibly control effort because structural properties have been tailored to augment the active control system. However, the vast majority of the work has used a series/sequential approach to arrive at an optimal design.

Scalar Approach

This integrated design task has almost exclusively been treated as a scalar optimization problem. The objective function is usually taken to be either: 1) the structural mass, with the other desired criteria (controller performance or system response characteristics) treated as constraints to define a feasible design space, or 2) a weighted sum of all desired properties and characteristics. In the first case, such an approach not only requires a priori determination of the criteria excluded from the objective function, but seriously weakens the overall design process by the choice of a single criterion to define the merit of an entire system. Design trade-offs may be accomplished (with some difficulty) by changing the constraints to define a new feasible design space and reaccomplishing the optimization problem.

In the second case, the combination of several conflicting, usually non-commensurable criteria which should be optimized simultaneously into a single scalar objective function is not only unnatural to the physics of the problem but also often inadequate. While commendable and significant in that structural and control syntheses are treated together vice sequentially, this combinatorial approach raises the question: what does minimization of a sum of structural properties (say mass) and controller characteristics

(say control energy or a steady-state linear quadratic regulator [LQR] cost function) really mean or represent? LQR controller synthesis suffers a similar identity crisis: why the minimization of a particular weighted integral of state and control variables? In the case of LQR controllers, the question is moot since the true motivation is to yield a tractable problem whose solution is readily synthesized and easily implemented. Likewise, the combinatorial approaches to structural/control design "represent at least a convenient parameterization of the problem wherein designs can be iteratively considered and improved through variation of the weighting matrices (1:1124)." Although doing such design sensitivity trade-offs only yields local information in the neighborhood of the optimum (2:483,503; 3:141; 4:1101; 5:333), this approach is particularly and conveniently amenable to solution via the vast software libraries of existing optimization techniques and algorithms.

Multiobjective Optimization

Multiobjective (multicriteria, multicriterion, vector) optimization is a more natural and, hopefully, more efficient approach to effectively account for the numerous different and often conflicting or competing criteria inherent in structural/control design problems. This approach may be mathematically considered as the vector extension of scalar optimization or, from an engineering point of view, seen as a tool to find compromise designs/solutions to the conflicting practical requirements. The designer can then systematically analyze the alternatives to arrive at a preferred solution which, while none of the criteria will necessarily attain its extremum, will satisfy the design requirements in some subjective 'best' way (2:503; 3:141; 4:1101).

Multiobjective optimization first arose in the study of mathematical economics and progressed to general decision-making and engineering (6:162-163; 7; 8; 9; 10; 11:1-10). Its use in structural mechanics dates back to the 1970's. Stadler's survey (12) examines

multicriteria optimization in the broader field of mechanics to 1984. Briefer summaries of its applications in structural mechanics to date are given by several authors (2:484; 3:141-142; 13:184; 14:119-120).

Pareto Optimality. (2:484-487; 3:142; 4:1102-1103; 5:333-334; 10:68-72; 15:925-926; 16:459-460). The general form of a multiobjective optimization problem is

$$\min_{\mathbf{z} \in \Omega} \boldsymbol{\gamma}(\mathbf{z}) \quad (2-1)$$

where $\boldsymbol{\gamma}: \Omega \rightarrow \Re^p$ is a vector objective function given by

$$\boldsymbol{\gamma}(\mathbf{z}) = [\gamma_1(\mathbf{z}), \gamma_2(\mathbf{z}), \dots, \gamma_p(\mathbf{z})]^T \quad (2-2)$$

The components $\gamma_i: \Omega \rightarrow \Re$, $i = 1, 2, \dots, p$ are the design criteria - the conflicting and often non-commensurable performance objectives. The design variable vector \mathbf{z} belongs to the feasible set $\Omega \subset \Re^d$, defined by

$$\Omega = \{ \mathbf{z} \in \Re^d : \mathbf{c}(\mathbf{z}) \leq 0, \mathbf{h}(\mathbf{z}) = 0 \} \quad (2-3)$$

where $\mathbf{c}_i: \Re^d \rightarrow \Re^r$, $i = 1, 2, \dots, r$ are inequality constraint functions and $\mathbf{h}_i: \Re^d \rightarrow \Re^q$, $i = 1, 2, \dots, q$ are equality constraint functions. The image of the feasible set in the criterion space is the attainable set, given by

$$\Theta = \{ \boldsymbol{\gamma}(\mathbf{z}) \in \Re^p : \mathbf{z} \in \Omega \} \quad (2-4)$$

Since the components γ_i of the objective vector are usually conflicting, an optimal solution (or superior solution), that is, a unique point or value of \mathbf{z} which will minimize all γ_i simultaneously, will not, in general, exist for the multiobjective problem. Attention is therefore commonly directed to Pareto optimum solutions (non-inferior solutions, non-dominated solutions, efficient solutions).

A vector $\underline{z}^* \in \Omega$ is (strongly) Pareto optimal if and only if there exists no $\underline{z} \in \Omega$ such that $\gamma_i(\underline{z}) \leq \gamma_i(\underline{z}^*)$, $i = 1, 2, \dots, p$ with $\gamma_j(\underline{z}) < \gamma_j(\underline{z}^*)$ for at least one j . Verbally, \underline{z}^* is Pareto optimal if there exists no feasible vector \underline{z} which would decrease some criterion without causing a simultaneous increase in at least one other criterion. In contrast, if all elements of the objective vector are simultaneously achievable, the solution is termed "dominated".

If Θ is non-empty closed and $\max \{ \gamma_i(\underline{z}) : \underline{z} \in \Theta \} < \infty$ for all i , then Ω has at least one (strongly) Pareto optimal solution. "Thus, a large class of multiobjective optimization problems in structural design may be expected to possess at least one non-dominated solution (16:460)." Whereas in scalar optimization one optimal solution is usually characteristic of a problem, a set or family of Pareto optimal solutions generally exist for a multiobjective optimization problem. Mathematically speaking, the multiobjective optimization problem is 'solved' once the Pareto optimal set is determined. Practically speaking, too many Pareto optimal solutions often exist, and it may be necessary to order or rank the set to determine a preferred solution.

While there is an extensive literature of models and methods to generate the Pareto optimal set and hence solve multiobjective optimization problems, the choice of which technique to use on a given problem is very subjective, especially for nonlinear, large dimensioned problems. There is no requirement to seek Pareto over dominated solutions; it has simply become common practice to do so when possible. If they can be found, the Pareto solutions can be claimed to be optimal in some subjective sense, whereas dominated solutions are only attainable. Unfortunately, there are very few direct precedents for the multiobjective optimization of large, actively controlled structures. Based on the work and conclusions of Rao and associates (13, 14, 17), utility function, goal programming and cooperative game theory methods appeared promising.

The utility function and goal programming methods both reduce the original multiobjective problem to a scalar optimization problem (primarily as a weighted sum of the individual design objectives). Minimizing the scalar objective naturally yields a Pareto solution (corresponding to the particular scalarization scheme, weighting, etc.). However, both of these methods had difficulty converging to a solution for the sub-problem of control system design (placing closed-loop eigenvalues) and would not converge to solutions for integrated structural/control design (reducing mass while placing closed-loop eigenvalues). Therefore, these relatively simple approaches were abandoned and, based on these experiences, cooperative game theory (a much more complicated and elegant scalarization scheme) was never attempted.

Minimum Correction Homotopy Approach. Junkins and associates have used a minimum correction homotopy (MCH) approach to multiobjective optimization which can preserve the vector nature of the competing design criteria (18-21). However, in three of the four works (18-20), only controller design objectives (state error energy, control energy, and a stability robustness measure) were considered in a sequential approach minimizing one criterion while holding the other two objectives to prescribed values in the neighborhood of their unconstrained minima. In the fourth work (21), the MCH algorithm was used to establish a feasible design point satisfying a constraint vector of desired closed-loop eigenvalues. A robustness measure (the sensitivity of the closed-loop eigenvalues with respect to variation of uncertain system parameters) was subsequently minimized.

While the most notable and honestly vector approaches to multiobjective optimization, these four studies (18-21) still lack two important considerations from the standpoint of integrated structural/control design. First, only control system design was considered, although one case is presented (21) where a structural design iteration was performed before the MCH approach was used to satisfy the constraint vector. Second,

the 'true' objectives are not dealt with directly as a vector. They are either dealt with in sequence as constraints (18-20) or 'after the fact' (21). Indeed, values for the final or 'true' objective (robustness) are not even reported in (21).

Given the convergence problems encountered with utility function and goal programming approaches to finding Pareto optimal solutions, the MCH approach was turned to next. A simple extension of the vector (objective) function in (21) to include structural mass (and later control effort) applied the MCH technique to the problem of integrated structural/control design.

Although Stadler reported "the most extensive use of multicriteria optimization has been made in optimal structural design (12:282)," the techniques encompassed by the topic of multiobjective optimization are only beginning to be considered for the simultaneous or integrated structural/control design problem. While again commendable unifications of structural and control design objectives, the work to date may still be classified as either a series/sequential approach (17-20) or reduction (via some weighting scheme) to a scalar optimization problem (13, 14, 17-20).

The MCH method differs from the traditional or standard multiobjective optimization techniques in two ways. First, dominated vice Pareto solutions are found; there is no trade-off amongst the competing design objectives to arrive at some "best" solution. The method converges rapidly to the objective vector as specified. Second, the vector nature of the objectives is preserved vice the more common reduction to a scalar optimization problem.

In spite of these differences, the topic of multiobjective optimization should include the MCH approach in its catalog of techniques. This research shows the approach's validity and great utility to extend multiobjective optimization to the problem of integrated structural/control design.

III. Problem Formulation

Consider the discretized linearized equations of vibrational motion for a controlled structural system, neglecting disturbances:

$$M \ddot{\underline{w}} + C \dot{\underline{w}} + K \underline{w} = B \underline{u} \quad (3-1)$$

where

- \underline{w} = n-vector of generalized coordinates
- \underline{u} = a-vector of control inputs
- M = nxn symmetric positive definite mass matrix
- C = nxn symmetric positive semidefinite damping matrix
- K = nxn symmetric positive semidefinite stiffness matrix
- B = nxa control influence matrix
- $(\dot{})$ = $d()/dt$

For direct output feedback control of such a system, let local position and velocity measurements, respectively, be denoted as:

$$\underline{y}_p = H_p \underline{w}, \quad \underline{y}_v = H_v \dot{\underline{w}} \quad (3-2)$$

Assuming s colocated position and velocity sensors, $H_p = H_v = H$ and is an $s \times n$ matrix describing sensor locations and orientations, while \underline{y}_p and \underline{y}_v are s -vectors.

The control \underline{u} is a linear combination of the outputs:

$$\begin{aligned} \underline{u} &= - [G_p \underline{y}_p + G_v \underline{y}_v] \\ &= - G_p H \underline{w} - G_v H \dot{\underline{w}} \end{aligned} \quad (3-3)$$

where G_p and G_v are constant axis gain matrices.

If proportional damping is assumed,

$$C = \alpha M + \beta K \quad (3-4)$$

where α and β are positive constants. If Eqs (3-3) and (3-4) are substituted into Eq (3-1), the closed-loop system is

$$M_{cl} \ddot{\underline{w}} + C_{cl} \dot{\underline{w}} + K_{cl} \underline{w} = 0 \quad (3-5)$$

where

$$M_{cl} = M, \quad C_{cl} = \alpha M + \beta K + B G_v H, \quad K_{cl} = K + B G_p H \quad (3-6)$$

The second-order system of Eq (3-5) can be written in first-order state-space form:

$$A \dot{\underline{x}} = T \underline{x} \quad (3-7)$$

where

$$\underline{x} = \begin{Bmatrix} \underline{w} \\ \dot{\underline{w}} \end{Bmatrix}, \quad A = \begin{bmatrix} M_{cl} & 0 \\ 0 & M_{cl} \end{bmatrix}, \quad T = \begin{bmatrix} 0 & M_{cl} \\ -K_{cl} & -C_{cl} \end{bmatrix} \quad (3-8)$$

or, more conveniently, as

$$\dot{\underline{x}} = A_{cl} \underline{x} \quad (3-9)$$

where, since $M_{cl} = M$ and with I an identity matrix,

$$A_{cl} = \begin{bmatrix} 0 & I \\ -M^{-1} K_{cl} & -M^{-1} C_{cl} \end{bmatrix} \quad (3-10)$$

The associated right and left eigenvalues and eigenvectors of A_{cl} are, respectively,

$$\lambda_i \underline{e}_i = A_{cl} \underline{e}_i, \quad \lambda_i \underline{f}_i = A_{cl}^T \underline{f}_i \quad i = 1, 2, \dots, 2n \quad (3-11)$$

Assuming all eigenvalues are distinct and, therefore, the eigenvectors are linearly independent, the eigenvectors are conventionally normalized as

$$\underline{f}_i^T \underline{e}_j = \delta_{ij}, \quad \underline{f}_i^T A_{cl} \underline{e}_j = \delta_{ij} \lambda_i \quad (3-12a)$$

or

$$F^T E = I, \quad F^T A_{cl} E = [\Lambda] \quad (3-12b)$$

where E and F are the right and left eigenvector matrices whose i th columns are the eigenvectors \underline{e}_i and \underline{f}_i , respectively, δ_{ij} is the Kronecker delta, and $[\Lambda]$ is a diagonal matrix of the eigenvalues $\lambda_1, \lambda_2, \dots, \lambda_{2n}$.

The closed-loop damping ratios ζ_i and damped frequencies ω_i are related to the in general complex conjugate pairs of closed-loop eigenvalues λ_i as

$$\zeta_i = -\sigma_i / (\sigma_i^2 + \omega_i^2)^{1/2}, \quad \lambda_i = \sigma_i \pm j \omega_i \quad i = 1, 2, \dots, n \quad (3-13)$$

The specific structural model and control system used in this research are described in the next chapter, leading to explicit expressions for the system matrices and state, output and control vectors.

IV. Model Description

Integrated structural/control design modifications to the Draper/RPL spacecraft model will be demonstrated herein. This model has been used to test and demonstrate hardware and control laws for maneuvering large flexible spacecraft. As shown in Figure 4-1, the configuration consists of a large central hub with four identical appendages/arms symmetrically cantilevered from the hub. Each arm is modeled as a continuous beam with a lumped mass at the end.

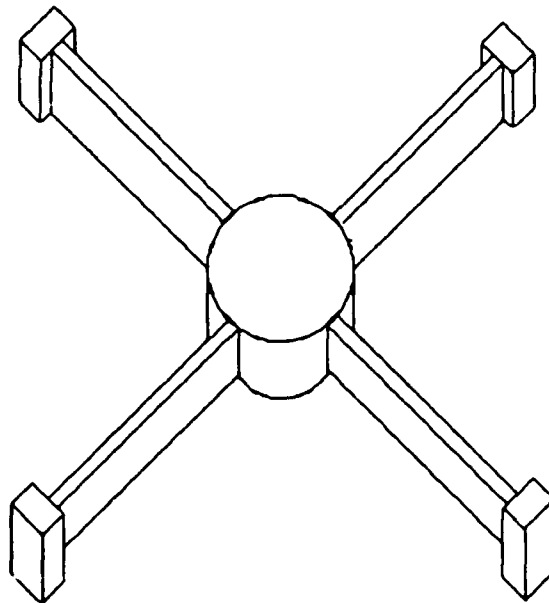


Figure 4-1. The Draper/RPL configuration

Vibrational Motion

Only the planar rotational and vibrational dynamics will be considered. Radial elongation of the arms and out-of-plane deformations are neglected. The equations of motion for the uncontrolled system are derived by finding the system kinetic and potential energies, using assumed modes to discretize the energies, truncating to second-order terms, forming the Lagrangian, and writing Lagrange's equations for the system. Figure 4-2 shows the Draper/RPL configuration with appendages numbered, deflections and rotations defined, and a body-fixed reference frame.

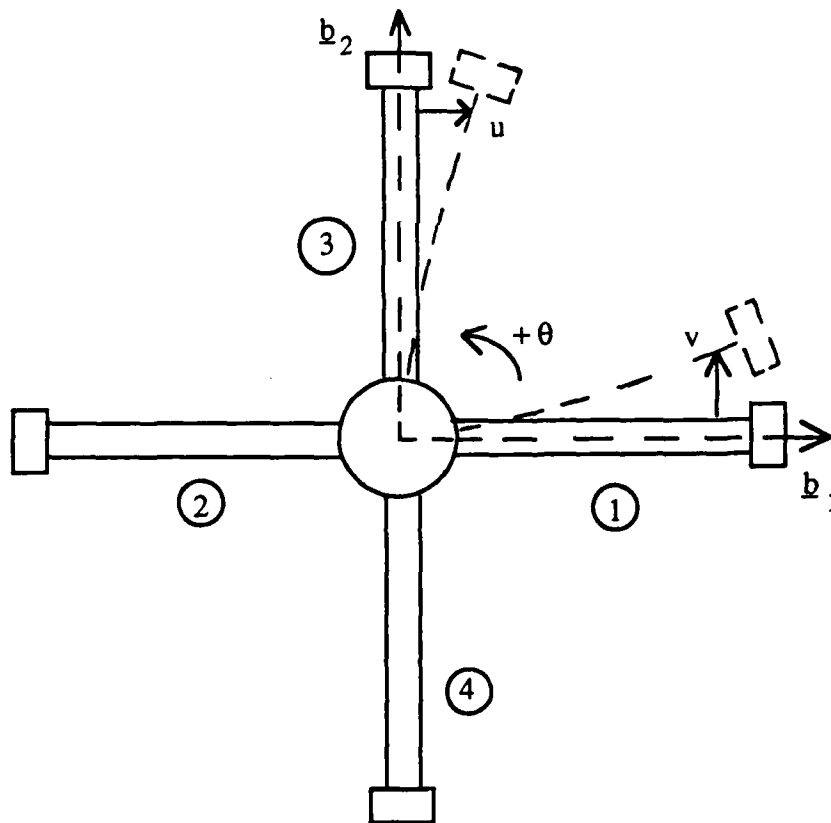


Figure 4-2. Draper/RPL configuration with reference frame and deflections defined

Kinetic Energy. The total kinetic energy will be written as the sum of the hub, appendage and tip mass energies.

The kinetic energy of the rigid hub alone is that of a solid cylinder:

$$T_h = \frac{1}{2} I_h \dot{\theta}^2 \quad (4-1)$$

where θ is the rigid-body rotation angle of the body-fixed reference frame with respect to an inertial reference frame, the hub moment of inertia is $I_h = m_h R^2 / 2$, m_h is the hub mass and R is the hub radius.

To determine the kinetic energy of appendage 1, a position vector is written as

$$\underline{r}_1 = x \underline{b}_1 + v \underline{b}_2 \quad (4-2)$$

The velocities of the elements of appendage 1 are obtained by taking the first time derivative of the position vector with respect to an inertial reference frame:

$$\begin{aligned} \dot{\underline{r}}_1 &= \dot{v} \underline{b}_2 + (\dot{\theta} \times \underline{r}_1) \\ &= -v \dot{\theta} \underline{b}_1 + (\dot{v} + x \dot{\theta}) \underline{b}_2 \end{aligned} \quad (4-3)$$

The \times denotes the outer or cross product. Finally, the kinetic energy of appendage 1 is the inner or dot product of the velocity vector with itself integrated with respect to the mass over the length of the appendage. Denoting the appendage's moment of inertia as

$$I_1 = \int_{x=R}^{x=R+L} x^2 dm \quad (4-4)$$

the kinetic energy of appendage 1 is

$$\begin{aligned}
 T_1 &= \frac{1}{2} \int_{x=R}^{x=R+L} (\dot{\mathbf{r}}_1 \cdot \dot{\mathbf{r}}_1) dm \\
 &= \frac{1}{2} \left\{ \left[\int_{x=R}^{x=R+L} (\dot{v}^2 + v^2 \dot{\theta}^2 + 2 \dot{v} \dot{\theta} x) dm \right] + I_1 \dot{\theta}^2 \right\} \quad (4-5)
 \end{aligned}$$

The kinetic energy of the tip mass on appendage 1 is found in a similar manner. The position vector is

$$\mathbf{r}_{t1} = (R+L) \mathbf{b}_1 + (v|_{x=R+L}) \mathbf{b}_2 \quad (4-6)$$

As a reminder that the deflection v must be evaluated at $x = R + L$, let $v_{t1} = v|_{x=R+L}$ and write the velocity vector as

$$\begin{aligned}
 \dot{\mathbf{r}}_{t1} &= \dot{v}_{t1} \mathbf{b}_2 + (\dot{\theta} \times \mathbf{r}_{t1}) \\
 &= -v_{t1} \dot{\theta} \mathbf{b}_1 + [\dot{v}_{t1} + \dot{\theta} (R+L)] \mathbf{b}_2 \quad (4-7)
 \end{aligned}$$

The velocity is then

$$\begin{aligned}
 V_{t1}^2 &= \dot{\mathbf{r}}_{t1} \cdot \dot{\mathbf{r}}_{t1} \\
 &= \dot{v}_{t1}^2 + 2 \dot{v}_{t1} \dot{\theta} (R+L) + \dot{\theta}^2 (R+L)^2 + v_{t1}^2 \dot{\theta}^2 \quad (4-8)
 \end{aligned}$$

To include the small effects of the rotary inertia of the tip mass, the angular velocity of the tip mass is that of the body-fixed reference frame plus a component due to the deflection of the end of the appendage (where the tip mass is located):

$$\begin{aligned}\dot{\theta}_{t1} &= \dot{\theta} + \frac{d\left(\frac{\delta v_{t1}}{\delta x}\right)}{dt} \\ &= \dot{\theta} + \dot{v}_{t1}'\end{aligned}\quad (4-9)$$

The kinetic energy of the tip mass is the sum of the translational and rotational energies:

$$T_{t1} = \frac{1}{2} [m_t V_{t1}^2 + I_t \dot{\theta}_{t1}^2] \quad (4-10)$$

The kinetic energy of appendage 3 and its tip mass are derived similarly:

$$T_3 = \frac{1}{2} \left\{ \left[\int_{y=R}^{y=R+L} (\dot{u}^2 + u^2 \dot{\theta}^2 + 2 \dot{u} \dot{\theta} y) dm \right] + I_3 \dot{\theta}^2 \right\} \quad (4-11)$$

$$T_{t3} = \frac{1}{2} [m_t V_{t3}^2 + I_t \dot{\theta}_{t3}^2] \quad (4-12)$$

where

$$I_3 = \int_{y=R}^{y=R+L} y^2 dm \quad (4-13a)$$

$$V_{t3}^2 = \dot{u}_{t3}^2 + 2 \dot{u}_{t3} \dot{\theta} (R+L) + \dot{\theta}^2 (R+L)^2 + u_{t3}^2 \dot{\theta}^2 \quad (4-13b)$$

$$\begin{aligned}\dot{\theta}_{t3} &= \dot{\theta} + \frac{d\left(\frac{\delta u_{t3}}{\delta y}\right)}{dt} \\ &= \dot{\theta} + \dot{u}_{t3}'\end{aligned}\quad (4-13c)$$

$$u_{t3} = u \big|_{y=R+L} \quad (4-13d)$$

Consider only the case of anti-symmetric deformations of the arms where $u_4 = -u_3$ and $v_2 = -v_1$, as shown in Figure 4-3.

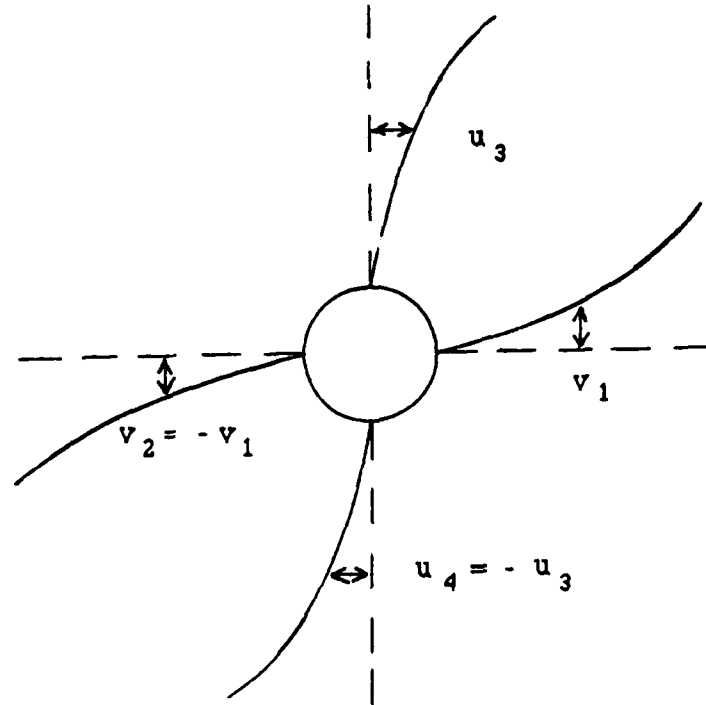


Figure 4-3. Anti-symmetric deformation

Thus, the kinetic energies of the first (third) appendage and tip mass are equal in magnitude to those of the second (fourth) appendages and tip mass - i.e., $T_2 = T_1$, $T_{t2} = T_{t1}$, $T_4 = T_3$, $T_{t4} = T_{t3}$. The total system kinetic energy (T) can be written as the sum of the individual energies:

$$T = T_h + 2(T_1 + T_{t1} + T_3 + T_{t3}) \quad (4-14)$$

To expand Eq (4-14), carry out the integrations over dm in the arm thickness (τ) and height (κ) dimensions, assume constant mass density along the arms (ρ_d), and noting that $I_3 = I_1$, define

$$I_0 = \frac{1}{2} I_h + 2 I_1 + 2 m_l (R + L)^2 \quad (4-15)$$

The total kinetic energy is then written as

$$\begin{aligned} T = & (I_0 + 2 I_1) \dot{\theta}^2 + \rho_d \tau \kappa \left[\int_R^{R+L} (\dot{v}^2 + v^2 \dot{\theta}^2 + 2 \dot{v} \dot{\theta} x) dx \right. \\ & \left. + \int_R^{R+L} (\dot{u}^2 + u^2 \dot{\theta}^2 + 2 \dot{u} \dot{\theta} y) dy \right] + I_1 [2 \dot{\theta} (\dot{v}'_{11} + \dot{u}'_{13}) + (\dot{v}'_{11})^2 + (\dot{u}'_{13})^2] \\ & + m_l [\dot{v}_{11}^2 + \dot{u}_{13}^2 + 2 \dot{\theta} (R+L) (\dot{v}_{11} + \dot{u}_{13}) + \dot{\theta}^2 (v_{11}^2 + u_{13}^2)] \quad (4-16) \end{aligned}$$

A discretized system model is formed by assuming that the elastic arm deformations (relative to a body-fixed undeformed state) can be represented as a linear combination of admissible (shape) functions $\mu_i(\rho)$ for the clamped-free appendage (21:699; 22:18):

$$\mu_i(\rho) = 1 - \cos(i\pi\rho/L) + 0.5(-1)^{i+1}(i\pi\rho/L)^2 \quad (4-17)$$

where π is the familiar mathematical constant, ρ is the radial distance along the arm (measured from the end clamped at the hub) and L is the arm length. This assumed mode or shape function must be an admissible function for the model of a continuous beam with a lumped mass at the end. The (shape) functions $\mu_i(\rho)$ are admissible since they satisfy the geometric boundary conditions of the appendage: $\mu(\rho=0) = 0$ since $u(t,0) = v(t,0) = 0$ and $\mu'(\rho=0) = 0$ since $u'(t,0) = v'(t,0) = 0$. [While not required, the $\mu_i(\rho)$ are also comparison functions for a clamped-free appendage (beam alone), since they also satisfy

the natural or physical boundary conditions: $\mu''(\rho=L) = 0$ since $u''(t,L) = v''(t,L) = 0$ and $\mu'''(\rho=L) = 0$ since $u'''(t,L) = v'''(t,L) = 0$. However, when the tip masses are included in the model, the $\mu_i(\rho)$ do not satisfy the natural boundary conditions but are still admissible functions.]

The transverse body-fixed deformations of the arms are modeled as

$$u(t, \rho) = \sum_{i=1}^{N_{sf}} U_i(t) \mu_i(\rho), \quad 0 \leq \rho \leq L \quad (4-18a)$$

$$v(t, \rho) = \sum_{i=1}^{N_{sf}} V_i(t) \mu_i(\rho), \quad 0 \leq \rho \leq L \quad (4-18b)$$

where N_{sf} is the number of admissible functions considered. This assumed-modes method yields a generalized parameter model with $U_i(t)$ and $V_i(t)$ the generalized displacement coordinates. Eqs (4-18) can be differentiated with respect to time and/or direction and substituted into the expression for the total system kinetic energy, Eq (4-16), to transform the expression to generalized coordinates.

Potential Energy. The potential energy of the system is the sum of the gravitational and strain energies. Since the structure is assumed to be in orbit (or, if on earth, supported by an air-bearing table), the gravitational potential will be neglected and the total potential energy P taken as the strain or elastic potential energy alone, summed over all four appendages:

$$P = E_y I_a \left[\int_0^L (u'')^2 d\rho + \int_0^L (v'')^2 d\rho \right] \quad (4-19)$$

E_y is the modulus of elasticity (Young's modulus), I_a is the area moment of inertia ($I_a = \kappa \tau^3/12$), and u'' and v'' are the second partial derivatives of $u(t, \rho)$ and $v(t, \rho)$ with respect to ρ . The restriction of anti-symmetric deformations also remains.

The assumed-modes method [Eqs (4-17) to (4-18)] again leads to the generalized parameter model with $U_i(t)$ and $V_i(t)$ the generalized displacement coordinates and $\mu_i(\rho)$ the admissible functions. Substituting into generalized parameters, differentiating and arranging in matrix notation yields

$$\begin{aligned} P = & E_y I_a \{U\}^T \left[\int_0^L \mu_i''(\rho) \mu_j''(\rho) d\rho \right] \{U\} \\ & + E_y I_a \{V\}^T \left[\int_0^L \mu_i''(\rho) \mu_j''(\rho) d\rho \right] \{V\} \end{aligned} \quad (4-20)$$

System Matrices. Now that the system kinetic and potential energies are in hand, the differential equations of motion are obtained from Lagrange's equation (for no nonconservative forces)

$$\frac{d}{dt} \left(\frac{\delta L_g}{\delta \dot{w}_i} \right) - \frac{\delta L_g}{\delta w_i} = 0 \quad (4-21)$$

where $i = 1, 2, \dots, \#$ of generalized coordinates. The Lagrangian is formed as $L_g = T - P$ where terms of order three or higher are neglected and the energies are written as

$$T = \frac{1}{2} \dot{\underline{w}}^T M \dot{\underline{w}} \quad (4-22a)$$

$$P = \frac{1}{2} \underline{w}^T K \underline{w} \quad (4-22b)$$

M and K are the mass and stiffness matrices, respectively [as shown in Eq (3-1)], and the vector of generalized coordinates is

$$\underline{x} = [\theta : U_1, U_2, \dots, U_{N_{sf}} : V_1, V_2, \dots, V_{N_{sf}}]^T \quad (4-23)$$

Assuming anti-symmetric appendage motion has reduced the number of generalized coordinates by $2 \times N_{sf}$. The order of the system of Eq (3-1) is thus $n = (2 \times N_{sf}) + 1$.

The elements of the mass and stiffness matrices are, for $i = 1, 2, \dots, N_{sf}$ and $j = 1, 2, \dots, N_{sf}$

$$M(1,1) = 2(I_0 + I_t) \quad (4-24a)$$

$$M(1, i+1) = 2 \left[m_2(R+L) \mu_i(L) + I_t \mu_i'(L) + \rho_d \tau \kappa \int_0^L (\rho + R) \mu_i(\rho) d\rho \right] \quad (4-24b)$$

$$M(i+1, j+1) = 2 \left[m_2 \mu_i(L) \mu_j(L) + I_t \mu_i'(L) \mu_j'(L) + \rho_d \tau \kappa \int_0^L \mu_i(\rho) \mu_j(\rho) d\rho \right] \quad (4-24c)$$

$$M(1, i+N_{sf}+1) = M(i+N_{sf}+1, 1) = M(i+1, 1) = M(1, i+1) \quad (4-24d)$$

$$M(i+N_{sf}+1, j+N_{sf}+1) = M(i+1, j+1) \quad (4-24e)$$

$$M(i+1, j+N_{sf}+1) = M(i+N_{sf}+1, j+1) = 0 \quad (4-24f)$$

$$K(i+1, j+1) = 2 E_y I_a \int_0^L \mu_i''(\rho) \mu_j''(\rho) d\rho \quad (4-25a)$$

$$K(i+N_{sf}+1, j+N_{sf}+1) = K(i+1, j+1) \quad (4-25b)$$

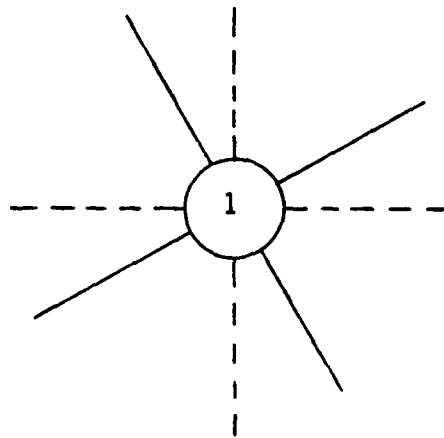
$$\begin{aligned} K(1,1) &= K(1, i+1) = K(1, i+N_{sf}+1) = K(i+1, 1) \\ &= K(i+N_{sf}+1, 1) = K(i+1, j+N_{sf}+1) \\ &= K(i+N_{sf}+1, j+1) = 0 \end{aligned} \quad (4-25c)$$

Model Order

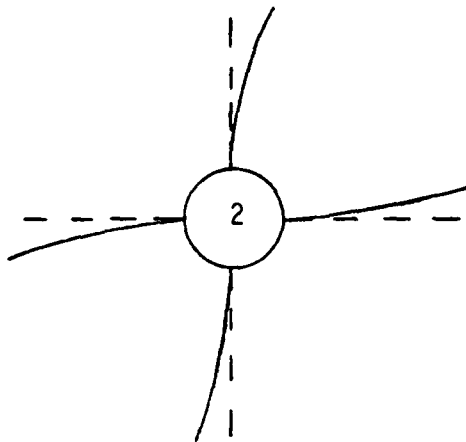
After the first (rigid-body) mode, conservation of angular momentum results in the vibrational modes occurring as pairs of 'opposition' and 'unison' modes. The first five normal modes are shown in Figure 4-4. The anti-symmetric 'opposition' modes are simple cantilever beam modes where adjacent arms move in opposition such that equal and opposite torques result in no hub (rigid-body) rotation. The anti-symmetric 'unison' modes are characterized by all four arms moving in unison; consequently, the hub rotates to conserve system angular momentum.

The frequencies of pairs of opposition and unison modes are closely spaced and aligned with the corresponding frequency of simple cantilever beam vibrations. This alignment and decrease in spacing with increasing mode number is shown in Table 4-1 for the first nine normal modes of the system (one rigid-body mode and four pairs of opposition/unison modes aligned with the first four cantilever beam modes).

Rigid-body mode



Opposition Mode



Unison Mode

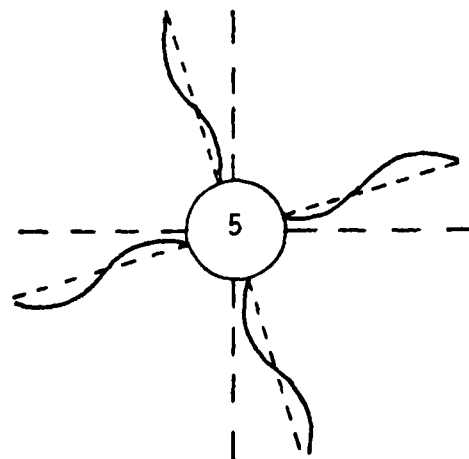
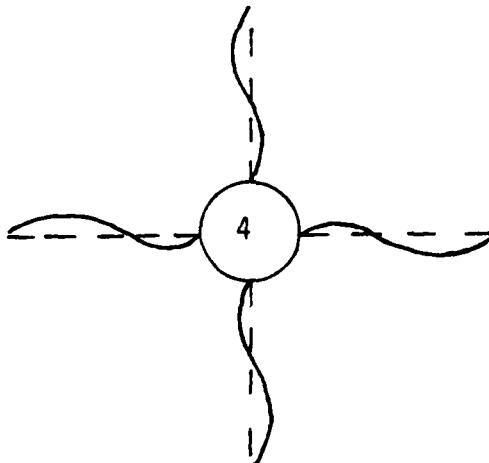
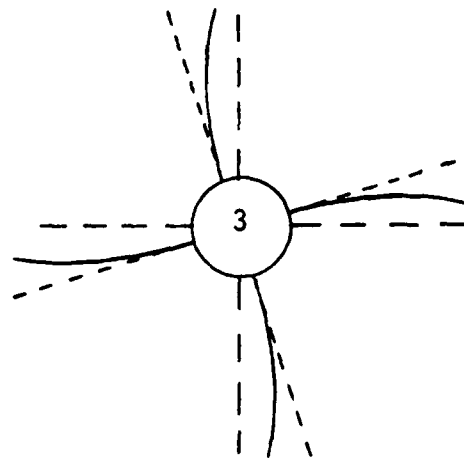


Figure 4-4. First five normal modes (21:700)

Table 4-1. Frequencies for first nine normal modes

| <u>Draper/RPL Structure</u> | | | <u>Cantilever Beam</u> | | |
|-----------------------------|------------------|-------------|------------------------|------------------|-------------|
| <u>Mode #</u> | <u>Frequency</u> | | <u>Mode #</u> | <u>Frequency</u> | |
| | <u>(Rad/sec)</u> | <u>(Hz)</u> | | <u>(Rad/sec)</u> | <u>(Hz)</u> |
| 1 | 0 | 0 | | | |
| 2 | 4.40 | 0.70 | | | |
| 3 | 7.92 | 1.26 | 1 | 9.42 | 1.50 |
| 4 | 51.46 | 8.19 | | | |
| 5 | 52.78 | 8.40 | 2 | 59.04 | 9.40 |
| 6 | 157.58 | 25.08 | | | |
| 7 | 158.34 | 25.20 | 3 | 165.33 | 26.31 |
| 8 | 313.09 | 49.83 | | | |
| 9 | 314.35 | 50.03 | 4 | 324.02 | 51.57 |

A typical design approach would begin with a very large-dimensional structural model, perhaps on the order of 100 modes or more, even when control of only a small number of lower modes is desired. Calculating and storing eigenvalues and eigenvectors (frequencies and mode shapes) for such a huge number of modes helps ensure the accuracy of the model at the lower modes by Rayleigh-Ritz convergence to the true mode shapes and frequencies from above. The model for control design is then a very accurate but truncated version of the much larger structural model. However, the desire in this research to integrate structural and control design precluded such an approach, as the basic structural parameters are to be design variables and iterated each loop along with the control system variables. Hence, a large-order structural model was not calculated and truncated to form a design model. The structural model will only include those modes to be controlled.

This research considers control system design by specifying damping ratios and frequencies of the first five normal modes, i.e., the rigid-body mode and the first two pairs of vibrational modes. Thus, $N_{sf} = 2$ and \underline{w} is a five-dimensional vector:

$$\underline{w} = [\theta, U_1, U_2, V_1, V_2]^T \quad (4-26)$$

Structural system design is accomplished by varying the thickness and height of the arms and hence structural mass. The arms are kept identical to each other as their dimensions are changed. The proportional damping constants in Eq (3-4) are taken to be $\alpha = 0$, $\beta = 10^{-5}$, so $C = 10^{-5} K$ and damping is proportional only to stiffness. With the values for the system parameters given in Table 4-2, the explicit expressions for the elements of the M and K matrices [Eqs (4-24) and (4-25)] can be evaluated.

Table 4-2. Draper/RPL configuration parameters

| | | |
|--------------------------------------|---------------------------|---|
| Hub radius (R) | 0.3048 m | (1 ft) |
| Rotary inertia of hub (I_h) | 10.8465 Kg-m ² | (8 slug-ft ²) |
| Mass density of arms (ρ_d) | 2,690 Kg/m ³ | (5.22 slug/ft ³) |
| Modulus of elasticity (E_y) | 7.584x10 ¹⁰ Pa | (1.584x10 ⁹ lb/ft ²) |
| Arm thickness (τ) | 0.003175 m | (0.0104166 ft) |
| Arm height (κ) | 0.1524 m | (0.5 ft) |
| Arm length (L) | 1.2192 m | (4.0 ft) |
| Tip mass (m_t) | 2.29038 Kg | (0.156941 slug) |
| Rotary inertia of tip mass (I_t) | 0.00244 Kg-m ² | (0.0018 slug-ft ²) |

Actuators and Sensors

Torque actuators are located on the central hub and at some position ρ_u on each arm. For a torque u_h at the hub, a torque u_1 at position ρ_{u1} on arms 1 and 2, and a torque u_2 at position ρ_{u2} on arms 3 and 4, the right-hand side of Eq (3-1) is

$$B \underline{u} = \begin{bmatrix} 1 & 2 & 2 \\ \underline{0} & 2 \underline{\mu}'(\rho_{u1}) & \underline{0} \\ \underline{0} & \underline{0} & 2 \underline{\mu}'(\rho_{u2}) \end{bmatrix} \begin{Bmatrix} u_h \\ u_1 \\ u_2 \end{Bmatrix} \quad (4-27)$$

where

$$\underline{\mu}'(\rho) = \frac{d}{d\rho} [\underline{\mu}(\rho)], \quad \underline{\mu}(\rho) = [\mu_1(\rho), \dots, \mu_{N_{sf}}(\rho)]^T \quad (4-28)$$

Angular position and angular velocity sensors are located on the hub, and colocated position and velocity sensors are placed at stations $\rho_{s1}, \rho_{s2}, \rho_{s3}, \rho_{s4}$ on arms 3 and 4 and stations $\rho_{s5}, \rho_{s6}, \rho_{s7}, \rho_{s8}$ on arms 1 and 2. The sensor influence matrix H is

$$H = \begin{bmatrix} 1 & \underline{0}^T & \underline{0}^T \\ 0 & \underline{\mu}^T(\rho_{s1}) & \underline{0}^T \\ \vdots & \vdots & \vdots \\ 0 & \underline{\mu}^T(\rho_{s4}) & \underline{0}^T \\ 0 & \underline{0}^T & \underline{\mu}^T(\rho_{s5}) \\ \vdots & \vdots & \vdots \\ 0 & \underline{0}^T & \underline{\mu}^T(\rho_{s8}) \end{bmatrix} \quad (4-29)$$

For the above configuration, then, $n = 5$ ($N_{sf} = 2$), $a = 3$ (actuators), $s = 9$ (sensors), B is a 5×3 ($n \times a$) matrix, and H is a 9×5 ($s \times n$) matrix. The gains G_p and G_v are both 3×9 ($a \times s$) matrices, and the output vectors are

$$\underline{y}_p = [\theta, u(t, \rho_{s1}), \dots, u(t, \rho_{s4}), v(t, \rho_{s5}), \dots, v(t, \rho_{s8})]^T \quad (4-30a)$$

$$\underline{y}_v = \dot{\underline{y}}_p \quad (4-30b)$$

The locations ρ_{u1} and ρ_{u2} of the torque actuators and $\rho_{s1}, \rho_{s2}, \dots, \rho_{s8}$ of the sensors will be allowed to vary during the design iterations to satisfy design objectives of placing closed-loop frequencies and damping ratios (ω and ζ) while achieving desired reductions in mass and/or control effort. Given the form Eq (3-3) of the control \underline{u} , the control effort v is defined as the Frobenius norm of the 10×10 ($2n \times 2n$) matrix G_{uu} given by

$$G_{uu} = \begin{bmatrix} H^T G_p^T G_p H & H^T G_p^T G_v H \\ H^T G_v^T G_p H & H^T G_v^T G_v H \end{bmatrix} \quad (4-31)$$

since

$$\underline{u}^T \underline{u} = \underline{x}^T G_{uu} \underline{x} \quad (4-32)$$

V. Optimization Technique

in order to do simultaneous (vice sequential) structure and control design, all desired objectives will be treated as elements of a vector vice being weighted and summed to form a scalar objective function. This vector approach precludes the use of existing, 'canned' optimization algorithms. Instead, a minimum correction homotopy (MCH) technique will be used (18-21, 23).

Minimum Correction Homotopy Algorithm

The p elements γ_i of the objective vector γ are the individual design objectives. The MCH algorithm solves the set of non-linear equations

$$\gamma_i^* (\underline{z}^*) - \gamma_i (\underline{z}) = 0 \quad i = 1, 2, \dots, p \quad (5-1)$$

where γ_i^* is the i th desired goal and \underline{z} is a d -vector of design variables. The first step is to generate a homotopy family of problems by introducing 'portable' goal function values defined by the linear map

$$\gamma_i^p(\alpha_H) = \alpha_H \gamma_i^* + (1 - \alpha_H) \gamma_i(\underline{z}_{\text{start}}) \quad i = 1, 2, \dots, p \quad (5-2)$$

with α_H the homotopy or continuation parameter. Replacing the original goals γ_i^* in Eq (5-1) with the goals $\gamma_i^p(\alpha_H)$ yields the homotopy family of non-linear equations

$$\gamma_i[\underline{z}(\alpha_H)] + \{ \gamma_i(\underline{z}_{\text{start}}) - \gamma_i^*(\underline{z}^*) \} \alpha_H = \gamma_i(\underline{z}_{\text{start}}) \quad i = 1, 2, \dots, p \quad (5-3)$$

At $\alpha_H = 0$, the solution to Eq (5-3) is $\underline{z} = \underline{z}_{\text{start}}$, and at $\alpha_H = 1$, Eq (5-3) becomes the original system of Eq (5-1). Therefore, the desired solution is $\underline{z}(\alpha_H = 1)$.

Note that if a solution is achieved at $\alpha_H = 1$, in multiobjective optimization terms the solution is dominated and not Pareto. Also notice that the second term on the left-hand side of Eq (5-3) (term in $\{ \}$) may be interpreted as a 'search direction' multiplied by a 'step size' (α_H). This formulation has favorable convergence characteristics since iterations can be started with close estimates of the solution vector $[z(\alpha_H)]$ at each continuation step as α_H is swept from zero to one. The 'step size' (increment in α_H) can also be changed adaptively in each iteration, an attractive feature for highly non-linear objective functions.

For a given continuation step, α_H , Eq (5-3) is usually underdetermined. A unique correction vector Δz is obtained by minimizing $\Delta z^T W_H \Delta z$ subject to the truncated Taylor series expansion of Eq (5-3),

$$J(z + \Delta z) = J(z) + \left[\frac{\delta J}{\delta z} \right] \Delta z = 0 \quad (5-4)$$

where W_H is an arbitrary weighting matrix and $J(z)$ is defined as

$$J_i [z(\alpha_H)] = \alpha_H \gamma_i^* (z^*) + (1 - \alpha_H) \gamma_i (z_{start}) - \gamma_i [z(\alpha_H)] \quad i = 1, 2, \dots, p \quad (5-5)$$

Conforming to the implicit local linearity assumptions, the weighted minimum norm correction vector is

$$\Delta z = -W_H^{-1} \left[\frac{\delta J}{\delta z} \right]^T \left\{ \left[\frac{\delta J}{\delta z} \right] W_H^{-1} \left[\frac{\delta J}{\delta z} \right]^T \right\}^{-1} J(z) \quad (5-6)$$

where the pxd locally evaluated Jacobian is

$$\left[\frac{\delta J}{\delta z} \right] = - \left[\frac{\delta \gamma}{\delta z} \right] \quad (5-7)$$

Starting with a neighboring solution at the previous step and using the above correction vector Δz , $z(\alpha_H)$ is refined recursively by

$$\underline{z}(\alpha_H)_{\text{new}} = \underline{z}(\alpha_H)_{\text{old}} + \Delta \underline{z} \quad (5-8)$$

until local convergence is achieved [Eq (5-3) is satisfied] for each α_H . This is an 'inner loop' on $\Delta \underline{z}$. Final convergence is obtained (an 'outer loop') by incrementing α_H after each local convergence until $\alpha_H = 1$. Table 5-1 summarizes the procedure.

This MCH algorithm has proven effective for eigenvalue placement problems and, by its inherent reliance upon neighboring solutions, is also attractive for systematically conducting trade studies or generating trade-off surfaces (18-21, 23). Junkins (24) also showed that this minimum norm correction technique is theoretically equivalent to the gradient projection formulation for constrained optimization problems.

Table 5-1. MCH procedure

| <u>Start</u> <u>Iteration at</u> | <u>Iterate Minimum</u> <u>Norm Correction</u> | | <u>To Obtain</u> |
|---|--|---------------|----------------------------------|
| $\underline{z}_{\text{start}} = \underline{z}(0)$ | $\underline{J}[\underline{z}(\alpha_{H1})] = 0$ | \rightarrow | $\underline{z}(\alpha_{H1})$ |
| $\underline{z}(\alpha_{H1})$ | $\underline{J}[\underline{z}(\alpha_{H2})] = 0$ | \rightarrow | $\underline{z}(\alpha_{H2})$ |
| . | . | | . |
| . | . | | . |
| . | . | | . |
| $\underline{z}(\alpha_{Hq-1})$ | $\underline{J}[\underline{z}(1)] = 0$ | \rightarrow | $\underline{z}(\alpha_{Hq} = 1)$ |

with $0 < \alpha_{H1} < \alpha_{H2} < \dots < \alpha_{Hq} = 1$

Vector Objective Function

The structural design objective is taken to be the mass of the arms, π , defined as the product of their thickness, height, length and mass density. Control design objectives are the closed-loop frequencies ω_i and damping ratios ζ_i of the first five modes (one rigid-body rotation and four vibration modes) as well as the control effort v . The composite objective vector is

$$\gamma = [\omega_1, \zeta_1, \omega_2, \zeta_2, \dots, \omega_5, \zeta_5, \pi, v]^T \quad (5-9)$$

The design variables are the arm thickness, height, actuator and sensor locations, and elements of the feedback gain matrices. The design vector z is

$$z = [\tau, \kappa, \rho_{u1}, \rho_{u2}, \rho_{s1}, \rho_{s2}, \dots, \rho_{s8}, G_p(1,1), G_p(1,2), \dots, G_p(1,9), G_p(2,1), \dots, G_p(3,9), G_v(1,1), G_v(1,2), \dots, G_v(1,9), G_v(2,1), \dots, G_v(3,9)]^T \quad (5-10)$$

The arm length, L , and tip mass, m_t , have also been included as design variables in previous studies (21, 22). They were not included as such in this research for two reasons: 1) they are more likely to be specified due to higher-level mission requirements, such as keeping some equipment away from the hub, while the arm thickness and height are more likely to be available as design options to support the tip masses, and 2) excluding arm length and tip mass reduced the dimensionality of the problem and the consequent computational burden without detracting from the utility and validity of the design method.

Results of studies with various combinations of the elements of γ will be presented in the next chapter.

Derivatives

As a matter of implementation, the full 12×66 (pxd) matrix $[\delta J / \delta z]$ was used in all design iterations, even though all $12 \gamma_i^*$ were not specified. The appropriate J_i were set to zero in Eq (5-6) to calculate correction vectors Δz . This was acceptable since dominated

solutions ($\alpha_H = 1$) were sought vice Pareto solutions, which seek zero gradients to maximize α_H . While more derivatives were calculated than necessary, all were obtained analytically (closed-form) vice numerically. If numerical differentiation had been required, the additional computational burden would have made it worthwhile to incorporate the logic to manipulate the matrices according to the specific objective vector under consideration.

To detail the derivatives, first expand the right-hand side of Eq (5-7) where the γ_i are as given in Eq (5-9):

$$\begin{bmatrix} \frac{\delta \gamma}{\delta z} \end{bmatrix} = \begin{bmatrix} \frac{\delta \gamma_1}{\delta z_1} & \frac{\delta \gamma_1}{\delta z_2} & \dots & \frac{\delta \gamma_1}{\delta z_d} \\ \frac{\delta \gamma_2}{\delta z_1} & \frac{\delta \gamma_2}{\delta z_2} & \dots & \frac{\delta \gamma_2}{\delta z_d} \\ \vdots & \vdots & \vdots & \vdots \\ \frac{\delta \gamma_p}{\delta z_1} & \frac{\delta \gamma_p}{\delta z_2} & \dots & \frac{\delta \gamma_p}{\delta z_d} \end{bmatrix} \quad (5-11)$$

Since $\pi = \rho_d \tau \kappa L$, the required derivatives are simply

$$\frac{\delta \gamma_{11}}{\delta z_1} = \frac{\delta \pi}{\delta \tau} = \rho_d \kappa L, \quad \frac{\delta \gamma_{11}}{\delta z_2} = \frac{\delta \pi}{\delta \kappa} = \rho_d \tau L \quad (5-12a)$$

$$\frac{\delta \gamma_{11}}{\delta z_i} = 0, \quad i = 2, 3, \dots, d = 66 \quad (5-12b)$$

For the rates of change of the closed-loop frequencies and damping ratios, recall Eq (3-13) and let z_k be any element of the design vector z :

$$\frac{\delta \lambda}{\delta z_k} = \frac{\delta \sigma}{\delta z_k} + i \frac{\delta \omega}{\delta z_k} \quad (5-13a)$$

$$\frac{\delta \zeta}{\delta z_k} = \frac{\omega \left[\sigma \left(\frac{\delta \omega}{\delta z_k} \right) - \omega \left(\frac{\delta \sigma}{\delta z_k} \right) \right]}{(\sigma^2 + \omega^2)^{3/2}} \quad (5-13b)$$

To obtain the $\delta \lambda / \delta z_k$, differentiation of Eq (3-12a) leads to, for $i = 1, 2, \dots, 2n$,

$$\frac{\delta \lambda_i}{\delta z_k} = \mathbf{f}_i^T \frac{\delta \mathbf{A}_{cl}}{\delta z_k} \mathbf{e}_i \quad (5-14)$$

Given the form of \mathbf{A}_{cl} in Eq (3-10),

$$\frac{\delta \mathbf{A}_{cl}}{\delta z_k} = \begin{bmatrix} 0 & 0 \\ \left[-\mathbf{M}^{-1} \left(\frac{\delta \mathbf{K}_{cl}}{\delta z_k} \right) \right] & \left[-\mathbf{M}^{-1} \left(\frac{\delta \mathbf{C}_{cl}}{\delta z_k} \right) \right] \\ \left[-\left(\frac{\delta \mathbf{M}^{-1}}{\delta z_k} \right) \mathbf{K}_{cl} \right] & \left[-\left(\frac{\delta \mathbf{M}^{-1}}{\delta z_k} \right) \mathbf{C}_{cl} \right] \end{bmatrix} \quad (5-15a)$$

$$\frac{\delta \mathbf{M}^{-1}}{\delta z_k} = -\mathbf{M}^{-1} \left(\frac{\delta \mathbf{M}}{\delta z_k} \right) \mathbf{M}^{-1} \quad (5-15b)$$

[\mathbf{K}_{cl} and \mathbf{C}_{cl} were defined in Eq (3-6)]. \mathbf{M} and \mathbf{K} are functions of τ and κ only (z_1 and z_2).

Recalling the symmetry of those matrices given in Eqs (4-24) and (4-25), the expressions for the non-zero derivatives are, for $i = 1, 2, \dots, N_{sf}$ and $j = 1, 2, \dots, N_{sf}$,

$$\frac{\delta M(1,1)}{\delta z_1} = \frac{4}{3} \rho_d \kappa I_1 \quad (5-16a)$$

$$\frac{\delta M(1, i+1)}{\delta z_1} = 2 \rho_d \kappa \int_0^L (\rho + R) \mu_i(\rho) d\rho \quad (5-16b)$$

$$\frac{\delta M(i+1, j+1)}{\delta z_1} = 2 \rho_d \kappa \int_0^L \mu_i(\rho) \mu_j(\rho) d\rho \quad (5-16c)$$

$$\frac{\delta K(i+1, j+1)}{\delta z_1} = \frac{1}{2} E_y \tau^2 \kappa \int_0^L \mu_i''(\rho) \mu_j''(\rho) d\rho \quad (5-16d)$$

$$\frac{\delta M(1,1)}{\delta z_2} = \frac{4}{3} \rho_d \tau I_1 \quad (5-17a)$$

$$\frac{\delta M(1, i+1)}{\delta z_2} = 2 \rho_d \tau \int_0^L (\rho + R) \mu_i(\rho) d\rho \quad (5-17b)$$

$$\frac{\delta M(i+1, j+1)}{\delta z_2} = 2 \rho_d \tau \int_0^L \mu_i(\rho) \mu_j(\rho) d\rho \quad (5-17c)$$

$$\frac{\delta K(i+1, j+1)}{\delta z_2} = \frac{1}{6} E_y \tau^3 \int_0^L \mu_i''(\rho) \mu_j''(\rho) d\rho \quad (5-17d)$$

The rest of the components of K_{cl} and C_{cl} are not functions of τ or κ . Recalling the definition of the design vector \underline{z} [Eq (5-10)],

$$B = B(\rho_{u1}, \rho_{u2}) = B(z_3, z_4) \quad (5-18a)$$

$$H = H(\rho_{s1}, \rho_{s2}, \dots, \rho_{s8}) = H(z_5, z_6, \dots, z_{12}) \quad (5-18b)$$

$$G_p = G_p(z_{13}, z_{14}, \dots, z_{39}) \quad (5-18c)$$

$$G_v = G_v(z_{40}, z_{41}, \dots, z_{66}) \quad (5-18d)$$

Given the forms of B and H [Eqs (4-27) to (4-29)], the only non-zero elements of $[\delta B/\delta z_k]$ and $[\delta H/\delta z_k]$ are in the positions corresponding to the particular z_k :

$$\frac{\delta B}{\delta z_k} = 2 \mu_i''(z_k), \quad k = 3, 4 \quad (5-19a)$$

$$\frac{\delta H}{\delta z_k} = \mu_i'(z_k), \quad k = 5, 6, \dots, 12 \quad (5-19b)$$

$$\mu_i'(\rho) = \frac{i\pi}{L} \left[(-1)^{i+1} \left(\frac{i\pi\rho}{L} \right) + \sin \left(\frac{i\pi\rho}{L} \right) \right] \quad (5-19c)$$

$$\mu_i''(\rho) = \left(\frac{i\pi}{L} \right)^2 \left[(-1)^{i+1} + \cos \left(\frac{i\pi\rho}{L} \right) \right] \quad (5-19d)$$

Note $i = 1, 2$ ($i = 1, 2, \dots, N_{sf}$; $N_{sf} = 2$) and π is the mathematical constant, not the arm mass, in Eqs (5-19).

Even more simply, the elements of $[\delta G_p/\delta z_k]$ and $[\delta G_v/\delta z_k]$ are all zeroes except for a one in the position corresponding to the particular z_k .

Finally, recalling the form of the control effort matrix G_{uu} [Eq (4-31)] and denoting the magnitude or Frobenius norm of G_{uu} as $\|G_{uu}\|$,

$$v = \|G_{uu}\| = \left\{ \sum_{i=1}^{2n=10} \sum_{j=1}^{2n=10} [G_{uu}(i,j)]^2 \right\}^{\frac{1}{2}} \quad (5-20a)$$

$$\frac{\delta v}{\delta z_k} = \frac{1}{v} \sum_{i=1}^{10} \sum_{j=1}^{10} G_{uu}(i,j) \left[\frac{\delta G_{uu}(i,j)}{\delta z_k} \right] \quad (5-20b)$$

Given the functional dependencies in Eqs (5-18) and the expressions for $[\delta H/\delta z_k]$ in Eqs (5-19b) and (5-19c), the elements of $[\delta G_{uu}/\delta z_k]$ are

$$\frac{\delta G_{uu}}{\delta z_k} = \begin{bmatrix} \left[\left(\frac{\delta H}{\delta z_k} \right)^T G_p^T G_p H + \left[\left(\frac{\delta H}{\delta z_k} \right)^T G_p^T G_v H + \right. \right. \\ \left. \left. H^T G_p^T G_p \left(\frac{\delta H}{\delta z_k} \right) \right] \right] & \left[\left(\frac{\delta H}{\delta z_k} \right)^T G_v^T G_v H + \left[\left(\frac{\delta H}{\delta z_k} \right)^T G_v^T G_p H + \right. \right. \\ \left. \left. H^T G_v^T G_p \left(\frac{\delta H}{\delta z_k} \right) \right] \right] & \left[\left(\frac{\delta H}{\delta z_k} \right)^T G_v^T G_v H + \left[\left(\frac{\delta H}{\delta z_k} \right)^T G_v^T G_p H + \right. \right. \\ \left. \left. H^T G_v^T G_p \left(\frac{\delta H}{\delta z_k} \right) \right] \right] & \left[\left(\frac{\delta H}{\delta z_k} \right)^T G_v^T G_v H + \left[\left(\frac{\delta H}{\delta z_k} \right)^T G_v^T G_p H + \right. \right. \\ \left. \left. H^T G_v^T G_p \left(\frac{\delta H}{\delta z_k} \right) \right] \right] \end{bmatrix}$$

$$k = 5, 6, \dots, 12 \quad (5-21a)$$

$$\frac{\delta G_{uu}}{\delta z_k} = \begin{bmatrix} \left[H^T \left\{ \left(\frac{\delta G_p}{\delta z_k} \right)^T G_p + G_p^T \left(\frac{\delta G_p}{\delta z_k} \right) \right\} H \right] & \left[H^T \left(\frac{\delta G_p}{\delta z_k} \right)^T G_v H \right] \\ \left[H^T G_v^T \left(\frac{\delta G_p}{\delta z_k} \right) H \right] & [0] \end{bmatrix}$$

$$k = 13, 14, \dots, 39 \quad (5-21b)$$

$$\frac{\delta G_{uu}}{\delta z_k} = \begin{bmatrix} [0] & \left[H^T G_p^T \left(\frac{\delta G_v}{\delta z_k} \right) H \right] \\ \left[H^T \left(\frac{\delta G_v}{\delta z_k} \right)^T G_p H \right] & \left[H^T \left\{ \left(\frac{\delta G_v}{\delta z_k} \right)^T G_v + G_v^T \left(\frac{\delta G_v}{\delta z_k} \right) \right\} H \right] \end{bmatrix}$$

$$k = 40, 41, \dots, 66 \quad (5-21c)$$

Design Procedure

Now that all necessary equations have been detailed, the following are the steps to go through one 'inner loop' of the design procedure (Table 5-1), starting with $\alpha_H = \alpha_{H1} = 0.1$.

1. Initialization - set constants, read initial variable values from input files, etc.
2. Calculate system matrices - M [Eqs (4-24)], K [Eqs (4-25)], B [Eqs (4-27), (4-28), (5-19c)], C [Eq (3-4)], H [Eqs (4-29), (4-17)], A_{cl} [Eqs (3-10), (3-6)].
3. Calculate right and left eigenvalues and eigenvectors of A_{cl} [Eq (3-11)]; sort in order of increasing frequency and normalize eigenvectors [Eq (3-12)].
4. Calculate objective vector γ [Eq (5-9)] - frequencies and damping ratios given by Eq (3-13), control effort v by Eqs (5-20a) and (4-31), and mass $\pi = \rho_d \tau \kappa L$.
5. Calculate gradients.
 - a. Partial derivatives of mass and stiffness matrices [Eqs (5-16) and (5-17)].
 - b. Partial derivatives of control and sensor influence matrices [Eqs (5-19)].
 - c. Partials of A_{cl} [Eqs (5-15), (3-6)].
 - d. Partials of closed-loop eigenvalues [Eq (5-14)].
 - e. Partials of closed-loop frequencies and damping ratios [Eqs (5-13)].

- f. Partial derivatives of mass [Eqs (5-12)].
- g. Partial derivatives of control effort [Eqs (5-20), (5-21), (4-31)].
- 6. Form gradient matrix $[\delta J / \delta \underline{z}]$ [Eqs (5-7), (5-11)] from results of steps (5-e) thru (5-g) above.
- 7. Calculate correction to design vector [Eqs (5-6), (5-5)].
- 8. Check that corrections $\Delta \underline{z}$ will not violate any constraints on elements of \underline{z} (for example: thickness, height, sensor and actuator locations). If any will be violated, augment \underline{J} with the amount(s) of the violation(s), augment $[\delta J / \delta \underline{z}]$ with a -1 in the appropriate location(s) [row(s) and column(s)], and re-calculate correction vector $\Delta \underline{z}$ as in step (7) above.
- 9. Calculate magnitude of correction vector ($|\Delta \underline{z}|$; square root of the sum of the squares of the elements).
- 10. If $|\Delta \underline{z}| \leq z_{tol}$ (convergence limit), this inner loop has converged [Eq (5-3) is satisfied at this value of α_H]. Increment α_H and begin new inner loop at step (7) above.
- 11. If inner loop has not converged, calculate new design vector \underline{z} [Eq (5-8)] and return to step (2) above for another iteration.

Once the inner loop has converged [step (10)] at $\alpha_H = 1$, the homotopy family of equations [Eq (5-3)] has become the original system of Eq (5-1), and the procedure has converged to the desired objective vector \underline{y}^* .

VI. Integrated Structural/Control Optimal Design Results

Two cases were considered, most readily characterized by the first mode eigenvalues. Case 1 is high frequency, low damping. Case 2 is low frequency, high damping. The desired ω_i^* and ζ_i^* were not specified for all five modes. The eigenvalue portions of the objective vectors for the two cases are

$$\text{Case 1: } \gamma_1^* = [\omega_1^* = 3 \text{ rad/sec, } \zeta_1^* = 0.03, \zeta_2^* = 0.03, \zeta_3^* = 0.03, \\ \zeta_4^* = 0.01, \zeta_5^* = 0.01]^T \quad (6-1)$$

$$\text{Case 2: } \gamma_2^* = [\omega_1^* = 0.3, \omega_2^* = 4.5, \omega_3^* = 8.3, \zeta_1^* = 0.7, \\ \zeta_2^* = 0.03, \zeta_3^* = 0.03, \zeta_4^* = 0.01, \zeta_5^* = 0.01]^T \quad (6-2)$$

Note that this is not pole placement but rather partial specification of the eigenvalues for the first five normal modes of vibration.

All elements of the gain matrices G_p and G_v were initially set to zero except for $G_p(1,1)$, which was set to 0.001 to prevent the rigid-body eigenvalue being identically zero. Initial actuator locations were $\rho_{u1} = \rho_{u2} = L/2$. Initial sensor locations were $\rho_{s1} = \rho_{s5} = L/4$, $\rho_{s2} = \rho_{s6} = L/2$, $\rho_{s3} = \rho_{s7} = 0.7L$, $\rho_{s4} = \rho_{s8} = 0.9L$. Structural parameters were as given in Table 4-2. For Case 2, the arm length and tip mass were adjusted to 1.12 m (3.67 ft) and 2.90 Kg (0.19871 slug), respectively, to place the second- and third-mode frequencies (21).

The weighting matrix W_H in Eq (5-6) was nominally set to the identity matrix. Typical step size and convergence limits were $\Delta\alpha_H = 0.1$, $\Delta z = 0.0001$. However, the step size, weights and limits on the sensor and actuator locations were varied to aid convergence, particularly for large mass and control effort reductions.

Four types of designs were accomplished: 1) (partial) eigenvalue placement [γ_1^* and γ_2^* as given in Eqs (6-1) and (6-2)], 2) eigenvalue placement with mass reduction, 3) eigenvalue placement with control effort reduction, and 4) eigenvalue placement with mass and control effort reduction. The same (partial) eigenvalue placement was used for all designs within each case. The designs are identified by case number (first digit) and amount of mass and/or control effort reduction. For example, design 1-Base is Case 1, baseline (no mass or control effort reduction), design 1-M10 is Case 1, 10% mass reduction, design 2-CE25 is Case 2, 25% control effort reduction, and design 2-MCE50 is Case 2, 50% mass and control effort reduction.

Final values for elements of the design vector \underline{z} are given in Appendices A (τ , κ , ρ_{u1} , ρ_{u2} , ρ_{s1} , ρ_{s1} , ..., ρ_{s8} for all designs) and B (elements of G_p and G_v for designs 1-Base, 1-M50, 1-CE50, 1-MCE50 and 2-MCE50). Appendix C details the weighting matrices W_H for all designs.

Eigenvalue Placement

While closed-loop frequencies and damping ratios are certainly not complete specifications of a control system, they are familiar, easily understood characteristics, particularly for top-level concerns of structure/controller interaction. Solely placing the frequencies and damping ratios [as given in Eqs (6-1) and (6-2)] was not the purpose of this research, but is common to all integrated structural/control designs. Designs 1-Base and 2-Base were accomplished for Cases 1 and 2, respectively, and the resulting control efforts v were calculated [Eqs (4-31) and (5-20a)] and taken as the baseline values [Case 1: 12,500; Case 2: 85]. Note that while v does not have a physical interpretation, such as torque, it is still a valid measure of the amount of control exerted by the system and, hence, relative comparisons of v are meaningful. Actual control torques require specification of the state vector.

Figures 6-1 and 6-2 are typical trajectories of the eigenvalues (Cases 1 and 2, respectively) during the optimization process as α_H was swept from $\alpha_H = 0$ ($z = z_{\text{start}}$) to $\alpha_H = 1$ ($z = z^*$). These trajectories are representative of those for all of the designs.

Mass Reduction

For integrated structural/control design, the previous (partial) eigenvalue placement is accomplished simultaneously with reduction of the arm mass, π . The objective vectors γ_1^* and γ_2^* were augmented with the desired arm mass, π^* . Mass reductions of 10, 25 and 50% were obtained while placing the closed-loop eigenvalues as specified in Eqs (6-1) and (6-2). Mass reductions beyond 50% were not attempted but are certainly possible up to that corresponding to minimum limits on the arm dimensions, albeit at the expense of higher control efforts. Control efforts for the reduced-mass designs were calculated and are tabulated in Table 6-1. As expected, maintaining the closed-loop characteristics while reducing arm mass generally requires more control effort, although design 1-M25 (Case 1, 25% mass reduction) is a fortunate exception, apparently due to more favorable sensor placements (Appendix A).

Control Effort Reduction

As a precursor to reducing both mass and control effort, control effort was reduced while holding the arm mass fixed. The objective vectors γ_1^* and γ_2^* were augmented with the desired control effort, v^* , and control effort reductions of 10, 25 and 50% of the appropriate baselines were obtained while placing the closed-loop eigenvalues as specified in Eqs (6-1) and (6-2). The reductions were accomplished primarily through sensor placement (Appendix A). Reductions beyond 50% were not attempted.

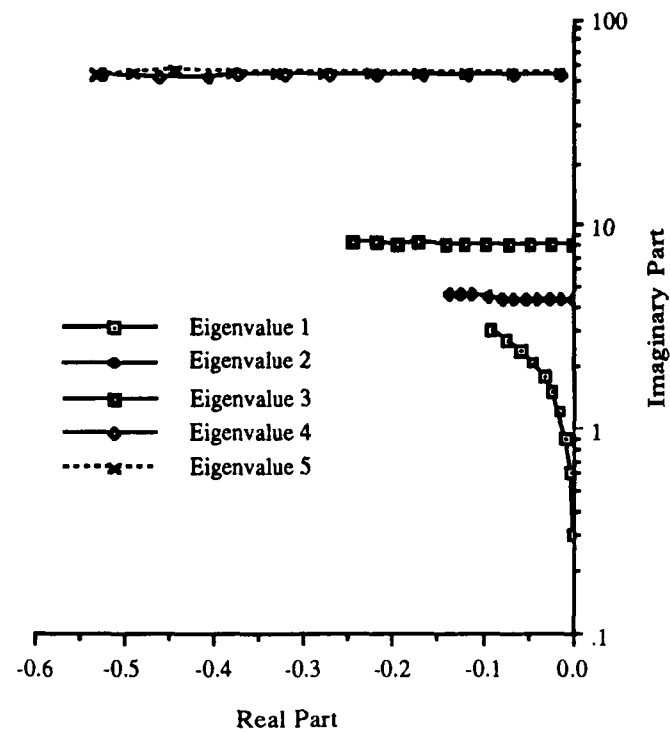


Figure 6-1. Case 1 eigenvalue trajectories

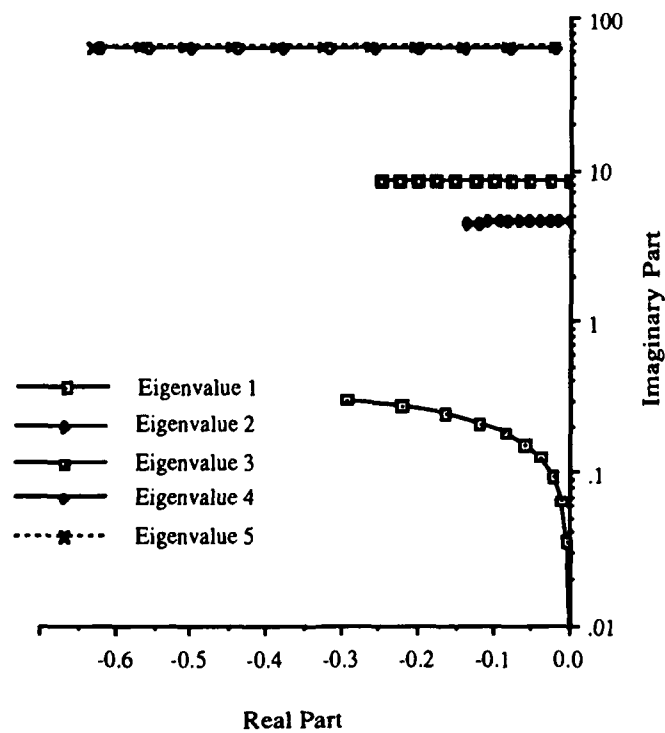


Figure 6-2. Case 2 eigenvalue trajectories

Table 6-1. Control efforts for reduced-mass designs

| Design # | % Mass Reduction | Control Effort ν |
|----------|------------------|----------------------|
| 1-Base | | 12,500 |
| 1-M10 | 10 | 13,500 |
| 1-M25 | 25 | 11,000 |
| 1-M50 | 50 | 32,400 |
| 2-Base | | 85 |
| 2-M10 | 10 | 339 |
| 2-M25 | 25 | 1,441 |
| 2-M50 | 50 | 4,323 |

Mass and Control Effort Reduction

Since the reduced-mass designs essentially assumed infinite available control effort, a more realistic problem is to augment the basic γ_1^* and γ_2^* with the desired arm mass and desired control effort. For Case 1, reductions of 10, 25 and 50% in both mass and control effort were obtained while placing the eigenvalues per Eq (6-1).

For Case 2, the arm length and tip mass had been adjusted to place the second- and third-mode frequencies (21) and the first-mode frequency is very low (0.3 rad/sec). Consequently, the baseline control effort (required to satisfy γ_2^*) is also very low, so low that only 5% reductions in mass and control effort could simultaneously be achieved (design 2-MCE5). Control efforts much larger than the baseline were required to satisfy eigenvalue placement with simultaneous mass reduction, as shown in Table 6-1. These control efforts were subsequently reduced by the same percentage as the mass, i.e., the control efforts corresponding to 10, 25 and 50% mass reductions were reduced by 10, 25 and 50%, respectively (designs 2-MCE10, 2-MCE25, 2-MCE50).

Spillover Sensitivity

Although design goals of mass and/or control effort were met while achieving desired closed-loop frequencies and damping ratios, the design model only included the first five normal modes. Model-order truncation, while a necessary evil for computational purposes, leaves the designs susceptible to spillover from the higher-order unmodeled or residual modes. All designs achieved previously (Appendix A) were evaluated against 7-, 9- and 11-mode evaluation models. Figures 6-3 through 6-7 are plots of the modes' damping ratio for designs 1-Base, 1-M50, 1-CE50, 1-MCE50 and 2-MCE50 (Case 1: baseline, 50% mass reduction, 50% control effort reduction, 50% mass and control effort reduction, and Case 2: 50% mass and control effort reduction) to show the extreme spillover sensitivity of the designs. The modes of the design model (1-5) are those whose damping ratios were specified during the design process. The 'baseline' damping (solid bar) is: 1) the specified damping ratio per Eq (6-1) for modes 1-5, and 2) the open-loop damping ratios for the residual modes (slightly stable due to the assumed proportional damping).

All the designs had at least one mode go unstable, while many unstable modes was more of the norm. Instability was not limited to the residual modes; modes in the design model were also driven unstable, as with modes 2 and 5 in Figure 6-6 and mode 4 in Figure 6-7. Even if the modes in the design model were not driven unstable, they were often subject to wild variations in damping ratio as soon as any higher-order modes were included in the evaluation model (modes 4 and 5 in Figure 6-5, mode 4 in Figure 6-6). There was no quantifiable correlation of spillover sensitivity with mass and/or control effort reduction, either within or across the two cases, other than all designs were very susceptible.

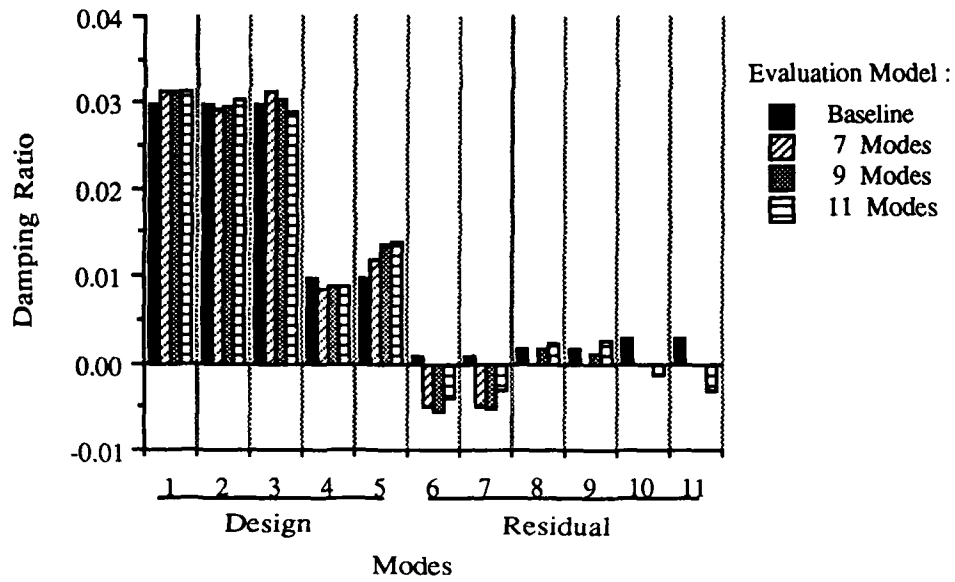


Figure 6-3. Damping ratio spillover sensitivity, design 1-Base
(Case 1, baseline)

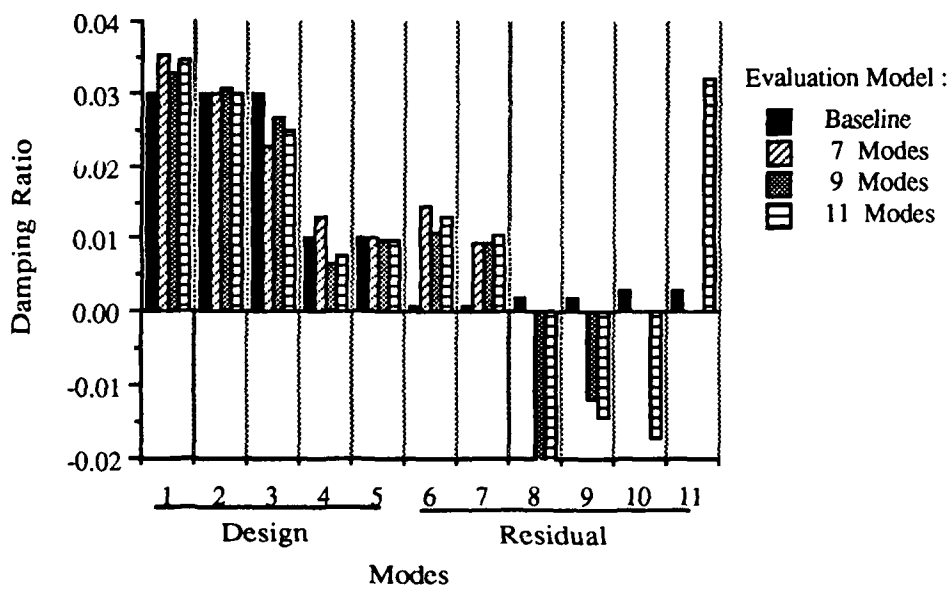


Figure 6-4. Damping ratio spillover sensitivity, design 1-M50
(Case 1, 50% mass reduction)

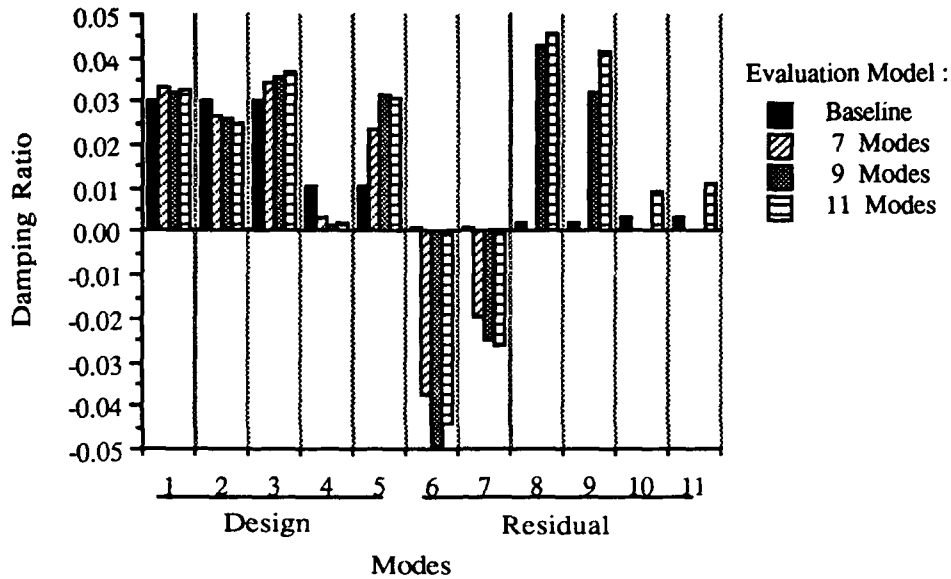


Figure 6-5. Damping ratio spillover sensitivity, design 1-CE50
(Case 1, 50% control effort reduction)

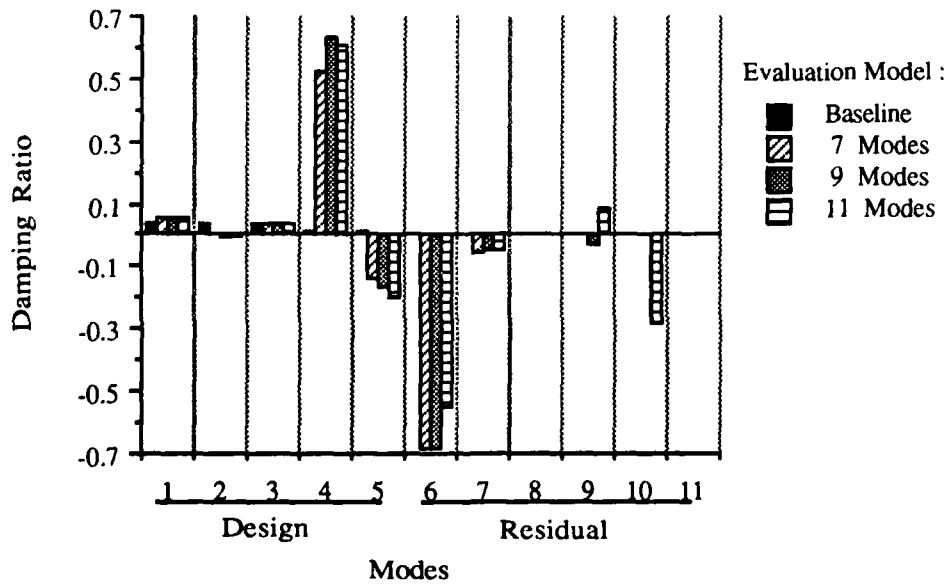


Figure 6-6. Damping ratio spillover sensitivity, design 1-MCE50
(Case 1, 50% mass and control effort reduction)

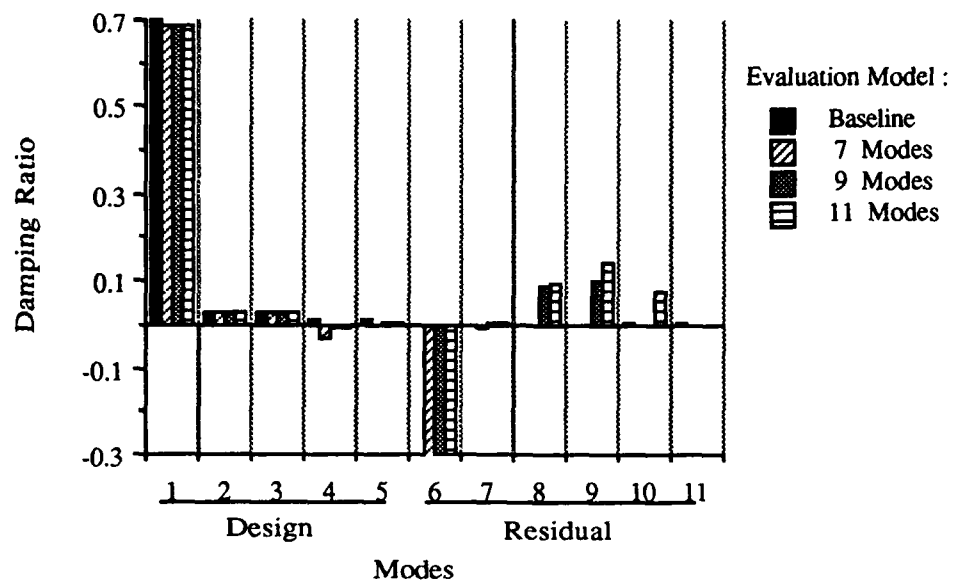


Figure 6-7. Damping ratio spillover sensitivity, design 2-MCE50
(Case 2, 50% mass and control effort reduction)

VII. Spillover Control

The minimum correction homotopy technique described in Chapter V has successfully been used for integrated structural/control design as evidenced by the designs achieved (listed in Appendix A). However, in light of the design model order truncation and lack of any robustness criteria in the design objective vector, the extreme spillover sensitivity of the designs is not surprising. Although spillover does not have to be destabilizing, it will certainly affect system performance. Thus, in order to provide a complete technique for integrated structural/control design, spillover control is also addressed. Two approaches were considered: simple constraints and modal suppression.

Constrained Solutions

The first approach to control spillover was simply to increase the order of the design model from 5 to 11 modes. No attempt was made to place the eigenvalues of the additional modes, 6-11; they were simply constrained to have damping ratios ≥ 0.001 . In effect, this was an attempt to simply meet the design objectives given in Chapter VI while guaranteeing stability through 11 modes; i.e., push off the onset of spillover to modes 12 and beyond, hoping that these much higher-frequency modes have less effect on the modes of the original design model (1-5). Or, it may be thought of as a 'brute force' attempt to build a deadband into the controller over the frequency range covered by modes 6-11 (~ 52-840 rad/sec).

As a matter of implementation, the objective vector was expanded to include the first 11 modes

$$\gamma = [\omega_1, \zeta_1, \omega_2, \zeta_2, \dots, \omega_{11}, \zeta_{11}, \pi, v]^T \quad (7-1)$$

[mass (π) and control effort (v) were included as appropriate]. Even though all 24 γ_i^* were not specified, the full 24x66 matrix $[\delta J/\delta z]$ was used in all design iterations. The appropriate J_i were set to zero in Eq (5-6) to calculate correction vectors Δz . Since this approach was only applied to the Case 1 designs, the J_i corresponding to $\omega_2, \omega_3, \dots, \omega_{11}$ were all set to zero. The spillover control then set the J_i corresponding to $\zeta_i, i = 6, 7, \dots, 11$ equal to zero if that ζ_i was ≥ 0.001 . Finally, design iterations were started with the 'converged' solutions from the Case 1 designs, i.e., the final designs were 'post-processed' to control spillover.

The new designs (with spillover control) were then evaluated against 13-, 15-, 17-, 19- and 21-mode evaluation models. Figures 7-1 and 7-2 are plots of the modes' damping ratios for designs 1-Base and 1-MCE50 (Case 1, baseline and Case 1, 50% mass and control effort reduction) with the spillover control included. Figure 7-1 (design 1-Base) shows the design stable and not too much variation in damping ratio through 21 modes. However, this design was the exception rather than the rule. The rest of the spillover-control designs exhibited characteristics similar to the non-spillover-control designs: all had multiple modes go unstable, including the spillover-controlled modes (6-11), and the damping ratios were often subject to wild variations with changing evaluation model size. The 25 and 50% mass and control effort reduction designs (1-MCE25, 1-MCE50) also had modes in the design model driven unstable (modes 2 and 5 in Figure 7-2).

In short, the simple constraint approach to spillover control did delay the onset of instability to modes 12 and higher, but the designs still exhibit far too much spillover sensitivity. Model-order truncation effects were not mitigated by this technique except for one fortunate design (1-Base), and that very exception points out the unreliability of this approach to control spillover.

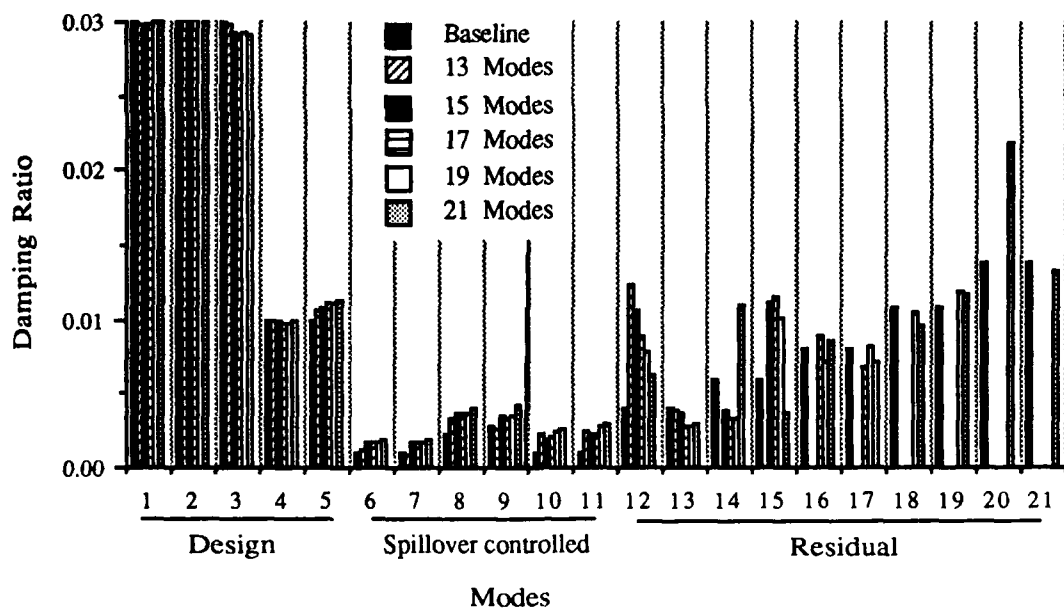


Figure 7-1. Damping ratio spillover sensitivity with simple constraint spillover control, design 1-Base (Case 1, baseline)

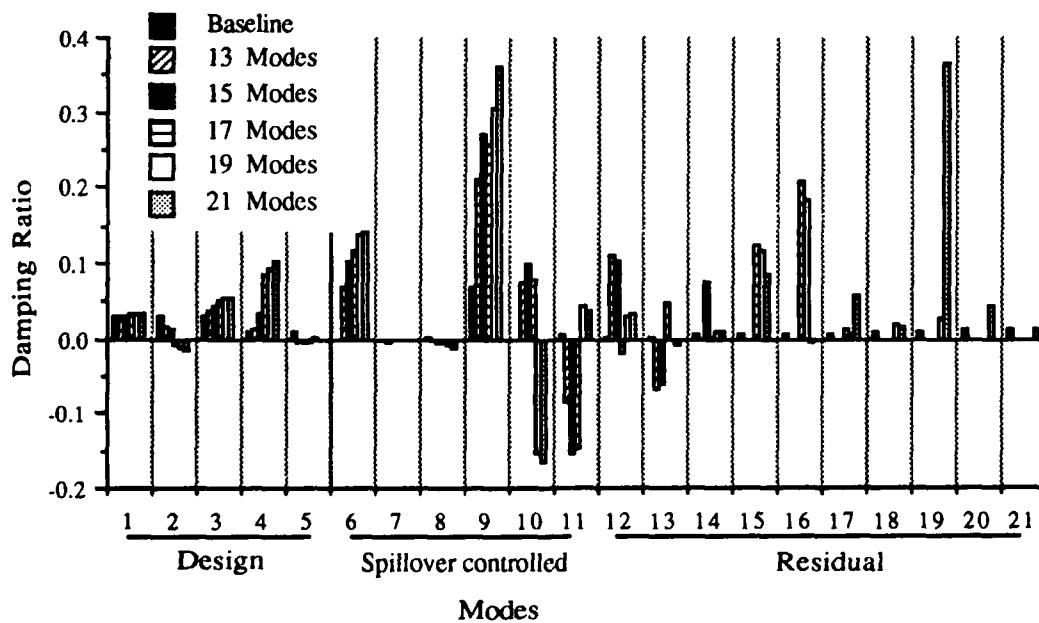


Figure 7-2. Damping ratio spillover sensitivity with simple constraint spillover control, design 1-MCE50 (Case 1, 50% mass and control effort reduction)

Modal Suppression

A modal suppression technique (25, 26) was attempted next. While the technique has also been used to design decoupled controllers (27-29), it is used here to eliminate observation spillover and recover stability.

Technique. Recalling the system of Eq (3-1), let ψ_i^2 and ϕ_i , $i = 1, 2, \dots, n$ be the eigenvalues and eigenvectors of the associated eigenvalue problem

$$\psi_i^2 M \phi_i = K \phi_i \quad (7-2)$$

Define Φ as the matrix with ϕ_i as the i th column, where the ϕ_i have been normalized with respect to the mass matrix,

$$\Phi^T M \Phi = I \quad (7-3)$$

i.e., Φ is the system modal matrix. Also define the coordinate transformation

$$\underline{w} = \Phi \underline{\eta} \quad (7-4)$$

where $\underline{\eta}$ is an n -vector of modal coordinates.

The second-order system of Eq (3-1) can now be written in first-order state-space form as

$$\dot{\underline{x}} = A \underline{x} + D \underline{u} \quad (7-5)$$

where

$$\underline{x} = \begin{Bmatrix} \underline{\eta} \\ \dot{\underline{\eta}} \end{Bmatrix}, \quad \dot{\underline{x}} = \begin{Bmatrix} \dot{\underline{\eta}} \\ \ddot{\underline{\eta}} \end{Bmatrix} \quad (7-6)$$

$$A = \begin{bmatrix} 0 & I \\ [-\psi^2] & [-2\xi\psi] \end{bmatrix} \quad (7-7)$$

$$D = \begin{bmatrix} 0 \\ \Phi^T B \end{bmatrix} \quad (7-8)$$

$[-\psi^2]$ is a diagonal matrix of open-loop modal frequencies squared, and $[-2\xi\psi]$ is a diagonal damping matrix. The output y and control u are

$$y = \begin{bmatrix} H\Phi & 0 \\ 0 & H\Phi \end{bmatrix} x \quad (7-9)$$

$$u = [G_p : G_v] y \quad (7-10)$$

To eliminate observation spillover, first define a new output q as

$$q = \Gamma y \quad (7-11)$$

The matrix Γ will be chosen such that q does not contain any information regarding modes to be suppressed, say modes 6-r. In other words, q will be a linear combination of the elements of the output y such that only modes 1-5 are observed. Since there are nine sensors ($s=9$), if five modes are to be controlled, a maximum of four modes can be suppressed (i.e., $r=9$, suppress modes 6-9). There must be as many independent 'sources of information' (elements of the new output q) as modes to be controlled.

The columns of $H\Phi$ correspond to observations of modes:

$$H\Phi = \Xi = [\Xi_1 : \Xi_2 : \dots : \Xi_9] \quad (7-12)$$

To suppress observations of modes 6-9, Γ must be such that

$$\Gamma [\Xi_6 : \Xi_7 : \Xi_8 : \Xi_9] = \Gamma \Xi_{6-9} = 0 \quad (7-13)$$

Singular value decomposition is used to determine the null space of Ξ_{6-9}^T and Γ solved for by transposing Eq (7-13)

$$\Xi_{6-9}^T \Gamma^T = 0 \quad (7-14)$$

The new control becomes

$$\begin{aligned} \underline{u} &= [G_p : G_v] \underline{q} = [G_p : G_v] \Gamma \underline{y} \\ &= [G_p : G_v] \begin{bmatrix} \Gamma \Xi & 0 \\ 0 & \Gamma \Xi \end{bmatrix} \underline{x} \end{aligned} \quad (7-15)$$

Note that the gain matrices G_p and G_v must be reduced in size accordingly. For suppression of modes 6-9, G_p and G_v are 3x5 matrices.

Results. The 'converged' solutions from eigenvalue placement, 50% mass reduction, 50% control effort reduction, and simultaneous 50% mass and control effort reduction were 'post-processed' to eliminate observation spillover: 1) structural sizes and sensor and actuator locations were held fixed, 2) Γ was calculated to suppress observation of modes 6-9, and 3) the MCH algorithm was re-run with the elements of the 3x5 G_p and G_v gain matrices the only variables adjusted to recover the closed-loop eigenvalue placement. Control effort was not specified [i.e., the desired objective vectors were as shown in Eqs (6-1) and (6-2), unaugmented] and the 5-mode design model was used.

Tables 7-1 through 7-3 detail the damping ratios obtained with up to a 19-mode evaluation model for designs 1-Base, 1-MCE50 and 2-MCE50 (Case 1, baseline; Case 1, 50% mass and control effort reduction; Case 2, 50% mass and control effort reduction).

However, all modal-suppression designs exhibit the same favorable characteristics. The controlled modes' (1-5) damping varies only slightly; there appears to be some 'conservation of damping ratio' within mode pairs (2&3, 4&5) at higher-order evaluations. The suppressed modes (6-9) remain at their open-loop damping ratios, as they should; since the controller can't 'see' those modes, it doesn't affect them. The assumed slight amount of proportional damping keeps modes 6-9 stable. Not only are the controlled and suppressed modes much more well-behaved, but the residual modes' (10-19) damping ratios are relatively immune to changes in the order of the evaluation model. There is now essentially one decade of deadband (modes 6-9, ~ 52 -530 rad/sec) above the controller bandwidth (modes 1-5, 0-52 rad/sec).

Two designs were also attempted suppressing only modes 6-7 (note G_p and G_v were 3×7 matrices). However, modes 8-10 remained unstable, whereas when modes 6-9 were suppressed, the onset of spillover instability was delayed until mode 1 at the earliest (for those two specific designs). As one might expect, making full use of the four extra sensors (suppressing modes 6-9) gave more robust designs than only putting in two modes of deadband (modes 6-7).

Finally, Table 7-3 shows the design stable through 19 modes. This fortunate (as opposed to planned) result points out the necessity to always check through all modes of interest to see if residual modes are stable or unstable - spillover does not necessarily always cause instability.

Table 7-1. Damping ratios with modal suppression, design 1-Base
(Case 1, baseline)

| <u>Mode #</u> | <u># of Modes in Evaluation Model</u> | | | | | |
|---------------|---------------------------------------|-----------|-----------|-----------|-----------|-----------|
| | 2 | 11 | 13 | 15 | 17 | 19 |
| 1 | 0.03 | 0.0299 | 0.03 | 0.0301 | 0.0301 | 0.0301 |
| 2 | 0.03 | 0.0299 | 0.03 | 0.03 | 0.03 | 0.03 |
| 3 | 0.03 | 0.0301 | 0.03 | 0.03 | 0.03 | 0.03 |
| 4 | 0.01 | 0.0106 | 0.0105 | 0.0104 | 0.0103 | 0.0102 |
| 5 | 0.01 | 0.00973 | 0.00978 | 0.00983 | 0.00985 | 0.00986 |
| 6 | 0.000799 | 0.000799 | 0.000799 | 0.000799 | 0.000799 | 0.000799 |
| 7 | 0.000803 | 0.000803 | 0.000803 | 0.000803 | 0.000803 | 0.000803 |
| 8 | 0.0016 | 0.0016 | 0.0016 | 0.0016 | 0.0016 | 0.0016 |
| 9 | 0.00161 | 0.00161 | 0.00161 | 0.00161 | 0.00161 | 0.00161 |
| 10 | | 0.0324 | 0.0327 | 0.0323 | 0.0322 | 0.032 |
| 11 | | 0.0357 | 0.0346 | 0.0349 | 0.035 | 0.0351 |
| 12 | | | 0.0166 | 0.0165 | 0.0164 | 0.0164 |
| 13 | | | -0.05 | -0.0499 | -0.0499 | -0.0496 |
| 14 | | | | -0.00609 | -0.00608 | -0.0066 |
| 15 | | | | -0.00788 | -0.00786 | -0.00751 |
| 16 | | | | | -0.00314 | -0.00314 |
| 17 | | | | | 0.00874 | 0.00875 |
| 18 | | | | | | -0.0287 |
| 19 | | | | | | 0.0141 |

Table 7-2. Damping ratios with modal suppression, design 1-MCE50
(Case 1, 50% mass and control effort reduction)

| <u>Mode #</u> | <u># of Modes in Evaluation Model</u> | | | | | |
|---------------|---------------------------------------|-----------|-----------|-----------|-----------|-----------|
| | 2 | 11 | 13 | 15 | 17 | 19 |
| 1 | 0.03 | 0.029 | 0.029 | 0.0292 | 0.0295 | 0.0295 |
| 2 | 0.03 | 0.0299 | 0.03 | 0.0298 | 0.0298 | 0.0297 |
| 3 | 0.03 | 0.0297 | 0.0296 | 0.0296 | 0.0296 | 0.0296 |
| 4 | 0.01 | 0.0113 | 0.0114 | 0.0113 | 0.0111 | 0.0111 |
| 5 | 0.01 | 0.00998 | 0.00998 | 0.00998 | 0.00998 | 0.00998 |
| 6 | 0.000867 | 0.000867 | 0.000867 | 0.000867 | 0.000867 | 0.000867 |
| 7 | 0.000869 | 0.000869 | 0.000869 | 0.000869 | 0.000869 | 0.000869 |
| 8 | 0.00171 | 0.00171 | 0.00171 | 0.00171 | 0.00171 | 0.00171 |
| 9 | 0.00172 | 0.00172 | 0.00172 | 0.00172 | 0.00172 | 0.00172 |
| 10 | | 0.0755 | 0.0756 | 0.0755 | 0.0753 | 0.0753 |
| 11 | | 0.00877 | 0.00876 | 0.00876 | 0.00876 | 0.00876 |
| 12 | | | 0.00609 | 0.006 | 0.00591 | 0.00591 |
| 13 | | | 0.00694 | 0.00703 | 0.00706 | 0.00708 |
| 14 | | | | 0.00443 | 0.00444 | 0.00444 |
| 15 | | | | -0.00784 | -0.00747 | -0.00753 |
| 16 | | | | | -0.035 | -0.0348 |
| 17 | | | | | 0.00924 | 0.00924 |
| 18 | | | | | | 0.0121 |
| 19 | | | | | | 0.0199 |

Table 7-3. Damping ratios with modal suppression, design 2-MCE50
(Case 2, 50% mass and control effort reduction)

| <u>Mode #</u> | <u># of Modes in Evaluation Model</u> | | | | | |
|---------------|---------------------------------------|-----------|-----------|-----------|-----------|-----------|
| | 2 | 11 | 13 | 15 | 17 | 19 |
| 1 | 0.7 | 0.699 | 0.7 | 0.7 | 0.7 | 0.7 |
| 2 | 0.03 | 0.0297 | 0.0298 | 0.0298 | 0.0298 | 0.0298 |
| 3 | 0.03 | 0.0306 | 0.0305 | 0.0304 | 0.0304 | 0.0305 |
| 4 | 0.01 | 0.00602 | 0.00642 | 0.00691 | 0.00657 | 0.00646 |
| 5 | 0.01 | 0.0138 | 0.0134 | 0.013 | 0.0133 | 0.0134 |
| 6 | 0.000958 | 0.000958 | 0.000958 | 0.000958 | 0.000958 | 0.000958 |
| 7 | 0.00096 | 0.00096 | 0.00096 | 0.00096 | 0.00096 | 0.00096 |
| 8 | 0.00189 | 0.00189 | 0.00189 | 0.00189 | 0.00189 | 0.00189 |
| 9 | 0.00189 | 0.00189 | 0.00189 | 0.00189 | 0.00189 | 0.00189 |
| 10 | | 0.00404 | 0.00406 | 0.00401 | 0.00407 | 0.0041 |
| 11 | | 0.00363 | 0.00355 | 0.00361 | 0.00354 | 0.00349 |
| 12 | | | 0.00554 | 0.00555 | 0.00557 | 0.00558 |
| 13 | | | 0.00563 | 0.00562 | 0.00561 | 0.0056 |
| 14 | | | | 0.007 | 0.00709 | 0.00712 |
| 15 | | | | 0.00723 | 0.00705 | 0.00697 |
| 16 | | | | | 0.0119 | 0.0121 |
| 17 | | | | | 0.0116 | 0.0115 |
| 18 | | | | | | 0.0149 |
| 19 | | | | | | 0.0151 |

VIII. Conclusions

This dissertation has presented an approach for integrated structural/control design and applied it to a flexible space structure (Draper/RPL configuration) and its active control system (direct output feedback). The primary contribution has been to treat the problem in an integrated or simultaneous fashion vice sequential design iterations on the two separate problems.

A minimum correction homotopy (MCH) technique was used to simultaneously optimize a vector of objective functions, including closed-loop damping ratios and frequencies, structural mass, and control effort. Hence, designs were achieved via multiobjective optimization vice forming a scalar objective via weighting and summing the individual objectives. The MCH technique has heretofore not been used to solve multiobjective optimization problems, nor has structural design (reduce mass) been combined with control system design at such a detailed level (place closed-loop frequencies and damping ratios, reduce control effort). [Note that the control system design was not pole placement, but specification of all damping ratios and some frequencies of interest, as shown in Eqs (6-1) and (6-2)].

Designs with up to 50% reductions in mass and/or control effort were obtained while achieving desired closed-loop characteristics for the first five normal modes of vibration. However, the designs, based on a reduced-order structural model, are easily driven unstable by spillover from higher-order unmodeled modes. A modal suppression technique completed the design approach by eliminating observation spillover from modes 6-9 and providing one decade of deadband above the controller bandwidth. The resultant designs are much less sensitive to the effects of model-order truncation. Additional deadband could easily be obtained by controlling fewer modes or simply adding sensors.

IX. Recommendations

The designs obtained in this research are dominated vice Pareto solutions. That is, all elements of the objective vector γ were simultaneously achievable; no trade-off amongst the elements of the objective vector (γ_i , individual objectives) was done to arrive at some subjective 'best' solution. Attempts to use both utility function and goal programming techniques as described in Chapter II to find Pareto optimal solutions to this multiobjective optimization problem were unsuccessful. In fact, mass and control effort were never included as objectives, since convergence for the sub-problem of eigenvalue placement was never achieved. A variety of weights and goals were tried, not only with closed-loop frequencies and damping ratios as design objectives but also using the real and imaginary parts of the closed-loop eigenvalues directly as the objectives in an attempt to at least reduce the nonlinearities of the problem, but all to no avail.

The first, natural extension of this research would be to use the minimum correction homotopy (MCH) design approach to find Pareto solutions. The reported body of research on multiobjective optimization and Pareto solutions, albeit not for integrated structural/control design but rather dealing with only one discipline, suggests utility function, goal programming, and/or game theory techniques (2-11, 13-17). Since all reported techniques involve some form of weighting and summing individual design objectives, direct application of the MCH algorithm may be difficult. However, given the excellent convergence characteristics of the MCH algorithm to dominated solutions, it seems worthwhile to attempt to use it to find Pareto solutions.

Whether dominated or Pareto solutions are sought, a valid question is: what are the best objective functions to use for integrated structural/control design? The design objectives used in this research (closed-loop frequencies and damping ratios, structural

mass, control effort), although certainly valid and important system characteristics, can certainly be improved upon. Additional objectives could be eigenvectors, robustness, structural stresses, displacements, etc. Any design improvements would then have to be weighed against the corresponding computational burdens and difficulties.

Any or all of the assumptions and parameters inherent in this proof-of-technique could be investigated. The design approach certainly needs to be examined with respect to much higher-dimensional problems, although no stumbling blocks other than computational loading are immediately foreseen. Using the technique with different structural models and/or control laws should not only verify the technique's utility and validity but also yield great varieties of design options and trade-offs.

Finally, the modal suppression technique could be incorporated into the main design iteration loop (vice being a 'post-processing' algorithm to recover stability) to see if such inclusion achieves required stability with lower control gains, control effort or sensitivity to uncertain parameters.

Appendix A: Final Design Vector Values

| Design | Arm Dimensions (ft) | | Locations non-dimensionalized by arm length (L) | | | | | | | | | | | | | | | |
|---------|------------------------|--------|---|-------------|-------------|-------------|-------------|-------------|-------------|-------------|-------------|-------------|--|--|--|--|--|--|
| | | | Actuators | | | | | | | | Sensors | | | | | | | |
| | I | K | ρ_{u1} | ρ_{u2} | ρ_{s1} | ρ_{s2} | ρ_{s3} | ρ_{s4} | ρ_{s5} | ρ_{s6} | ρ_{s7} | ρ_{s8} | | | | | | |
| 1-Base | 0.01055 | 0.4934 | 0.255 | 0.972 | 0.398 | 0.434 | 0.707 | 0.972 | 0.400 | 0.508 | 0.600 | 0.875 | | | | | | |
| 1-M10 | 0.01096 | 0.4277 | 0.969 | 0.969 | 0.368 | 0.400 | 0.601 | 0.972 | 0.363 | 0.400 | 0.605 | 0.952 | | | | | | |
| 1-M25 | 0.01168 | 0.3346 | 0.974 | 0.974 | 0.349 | 0.430 | 0.672 | 0.956 | 0.357 | 0.427 | 0.665 | 0.948 | | | | | | |
| 1-M50 | 0.01127 | 0.2310 | 0.978 | 0.977 | 0.272 | 0.136 | 0.313 | 0.901 | 0.528 | 0.450 | 0.583 | 0.967 | | | | | | |
| 1-CE10 | 0.01036 | 0.5020 | 0.350 | 0.962 | 0.406 | 0.272 | 0.373 | 0.642 | 0.639 | 0.669 | 0.519 | 0.446 | | | | | | |
| 1-CE25 | 0.01038 | 0.5011 | 0.348 | 0.966 | 0.397 | 0.283 | 0.358 | 0.642 | 0.605 | 0.630 | 0.513 | 0.441 | | | | | | |
| 1-CE50 | 0.01059 | 0.4916 | 0.374 | 0.972 | 0.424 | 0.282 | 0.374 | 0.572 | 0.557 | 0.593 | 0.380 | 0.427 | | | | | | |
| 1-MCE10 | 0.01100 | 0.4261 | 0.513 | 0.063 | 0.407 | 0.458 | 0.318 | 0.642 | 0.188 | 0.350 | 0.127 | 0.208 | | | | | | |
| 1-MCE25 | 0.01052 | 0.3713 | 0.412 | 0.979 | 0.458 | 0.526 | 0.526 | 0.739 | 0.024 | 0.702 | 0.547 | 0.509 | | | | | | |
| 1-MCE50 | 0.01207 | 0.2158 | 0.978 | 0.550 | 0.477 | 0.477 | 0.607 | 0.931 | 0.423 | 0.415 | 0.635 | 0.890 | | | | | | |
| 2-Base | 0.01042 | 0.4998 | 0.556 | 0.535 | 0.288 | 0.499 | 0.625 | 0.909 | 0.272 | 0.503 | 0.651 | 0.873 | | | | | | |
| 2-M10 | 0.01053 | 0.4450 | 0.784 | 0.792 | 0.316 | 0.470 | 0.600 | 0.820 | 0.324 | 0.478 | 0.600 | 0.842 | | | | | | |
| 2-M25 | 0.01076 | 0.3631 | 0.979 | 0.550 | 0.399 | 0.444 | 0.601 | 0.801 | 0.398 | 0.435 | 0.600 | 0.801 | | | | | | |
| 2-M50 | 0.01132 | 0.2300 | 0.972 | 0.964 | 0.416 | 0.489 | 0.509 | 0.567 | 0.409 | 0.510 | 0.546 | 0.634 | | | | | | |
| 2-CE10 | 0.01042 | 0.4998 | 0.553 | 0.535 | 0.307 | 0.500 | 0.601 | 0.907 | 0.275 | 0.495 | 0.633 | 0.855 | | | | | | |
| 2-CE25 | 0.01042 | 0.4998 | 0.554 | 0.536 | 0.329 | 0.500 | 0.578 | 0.922 | 0.285 | 0.495 | 0.618 | 0.861 | | | | | | |
| 2-CE50 | 0.01041 | 0.5003 | 0.039 | 0.546 | 0.400 | 0.461 | 0.503 | 0.851 | 0.228 | 0.416 | 0.408 | 0.390 | | | | | | |
| 2-MCE5 | 0.01044 | 0.4740 | 0.546 | 0.555 | 0.469 | 0.508 | 0.515 | 0.979 | 0.450 | 0.508 | 0.521 | 0.972 | | | | | | |
| 2-MCE10 | 0.01046 | 0.4479 | 0.555 | 0.546 | 0.474 | 0.492 | 0.492 | 0.929 | 0.466 | 0.484 | 0.486 | 0.864 | | | | | | |
| 2-MCE25 | 0.01080 | 0.3618 | 0.945 | 0.950 | 0.418 | 0.466 | 0.491 | 0.626 | 0.411 | 0.433 | 0.458 | 0.748 | | | | | | |
| 2-MCE50 | 0.01153 | 0.2259 | 0.980 | 0.980 | 0.371 | 0.385 | 0.374 | 0.509 | 0.361 | 0.378 | 0.379 | 0.527 | | | | | | |

Appendix B: Final Design Gains

Design 1-Base

| | | | | | | | | | | |
|-------|---|-------|--------|--------|--------|--------|--------|--------|-------|--------|
| G_p | = | 21.1 | -1.80 | -3.03 | -2.43 | 0.262 | -1.93 | -2.90 | -2.60 | -0.634 |
| | | 36.4 | -0.748 | -0.885 | 0.340 | 1.92 | -1.63 | -2.64 | -2.95 | -3.55 |
| | | 42.7 | -0.207 | -0.143 | 0.647 | 1.53 | 4.13 | 5.01 | 3.71 | -1.89 |
| G_v | | 0.800 | -0.746 | -1.04 | -0.747 | 0.209 | -0.807 | -0.919 | -1.13 | -0.991 |
| | = | 0.283 | -0.069 | -0.118 | 0.117 | 0.530 | -0.293 | -0.260 | 0.060 | 1.08 |
| | | 0.719 | 0.146 | 0.128 | -0.199 | -0.467 | 0.041 | -0.026 | 0.036 | -0.055 |

Design 1-M50

| | | | | | | | | | | |
|-------|---|--------|--------|--------|--------|--------|--------|-------|--------|--------|
| G_p | | 16.5 | -2.02 | -2.78 | -3.09 | -2.57 | -2.83 | -3.24 | -3.55 | -3.52 |
| | = | 27.8 | 1.91 | 2.53 | 2.94 | 2.45 | 0.031 | 1.80 | -0.700 | -3.92 |
| | | 26.2 | 0.470 | 1.58 | 0.448 | -2.80 | 3.02 | 3.84 | 3.89 | 3.62 |
| G_v | | 0.971 | -0.228 | -0.179 | -0.386 | -0.517 | -0.958 | -1.41 | -1.21 | -0.799 |
| | = | -0.928 | -0.034 | 0.037 | 0.302 | 0.044 | 0.435 | 0.161 | -0.461 | 0.758 |
| | | 0.622 | 0.021 | -1.15 | -1.02 | -0.444 | -0.993 | 0.213 | 0.599 | -0.329 |

Design 1-CE50

| | | | | | | | | | | |
|-------|---|-------|--------|--------|--------|--------|--------|--------|--------|--------|
| G_p | = | 20.5 | -2.04 | -2.90 | -2.68 | -0.453 | -2.43 | -3.24 | -3.15 | -2.37 |
| | | 37.2 | -1.98 | -1.81 | -2.25 | -1.18 | -1.20 | -3.05 | -1.76 | -0.034 |
| | | 38.2 | -0.029 | 0.935 | 1.30 | 1.08 | 2.01 | 3.54 | 3.73 | 2.34 |
| G_v | | 0.934 | 0.972 | 0.678 | 0.525 | 1.20 | -0.819 | -0.644 | -0.757 | -0.548 |
| | = | 2.69 | -0.372 | -0.309 | -0.026 | 0.606 | -1.69 | -0.755 | -1.17 | -0.794 |
| | | -2.64 | -1.92 | -1.24 | -1.26 | 2.93 | 0.074 | 0.516 | -0.365 | -0.707 |

Design 1-MCE50

| | | | | | | | | | | |
|-------|---|--------|--------|-------|--------|--------|--------|--------|--------|--------|
| G_p | | 19.0 | -1.99 | -2.89 | -2.14 | 0.926 | -2.39 | -3.31 | -2.65 | 0.355 |
| | = | 26.8 | 6.91 | 9.17 | 6.41 | -4.52 | -1.05 | 0.196 | -0.844 | -1.46 |
| | | 26.3 | -0.965 | 0.304 | -1.02 | -2.35 | 4.48 | 6.72 | 4.31 | -3.37 |
| G_v | | 0.101 | 0.747 | 0.701 | 0.685 | -0.042 | -0.071 | -0.113 | -0.312 | -0.691 |
| | = | -0.517 | 0.245 | 0.240 | -0.176 | -1.56 | -0.172 | -0.161 | 0.406 | 1.82 |
| | | 4.33 | -3.26 | -3.40 | -2.58 | 2.32 | 1.84 | 2.13 | 1.86 | -0.123 |

Design 2-MCE50

| | | | | | | | | | | |
|-------|---|-------|--------|--------|--------|--------|--------|--------|--------|--------|
| G_p | = | 2.60 | -0.264 | -0.451 | -0.530 | -0.122 | -0.387 | -0.571 | -0.662 | -0.366 |
| | | 0.536 | 3.56 | 4.42 | 4.72 | 4.36 | 0.478 | 1.50 | 0.559 | -2.25 |
| | | 0.620 | 0.980 | 1.99 | 1.06 | -1.71 | 3.16 | 4.00 | 4.29 | 3.88 |
| G_v | = | 3.04 | -0.835 | -0.957 | -0.989 | -1.41 | -1.96 | -2.06 | -2.13 | -2.76 |
| | | 3.23 | -0.263 | 0.008 | -0.005 | 1.54 | 0.451 | 0.375 | 0.412 | 0.402 |
| | | 4.30 | -0.034 | -0.129 | -0.160 | -1.07 | -1.19 | -0.954 | -0.945 | 1.06 |

Design 1-Base with modal suppression

| | | | | | | |
|-------|---|--------|--------|-------|--------|--------|
| G_p | = | -20.9 | -0.344 | -1.80 | -2.30 | -1.02 |
| | | -37.3 | -0.929 | -6.16 | -7.69 | -3.82 |
| | | -43.7 | 1.67 | 2.36 | 3.74 | 1.38 |
| G_v | = | -0.490 | 1.39 | 0.138 | -1.24 | 0.471 |
| | | 0.075 | 2.24 | 2.15 | -0.748 | -0.394 |
| | | -2.87 | 0.691 | -1.15 | 1.10 | -0.361 |

Design 1-M50 with modal suppression

| | | | | | | |
|-------|---|--------|--------|--------|--------|--------|
| G_p | = | -16.4 | -0.286 | -2.27 | -0.729 | -4.25 |
| | | -27.1 | 0.353 | 0.747 | 0.363 | -3.58 |
| | | -25.7 | -0.471 | 1.64 | 0.127 | 4.28 |
| G_v | = | -1.38 | -0.519 | -0.474 | -1.15 | -1.91 |
| | | 0.862 | 0.110 | 0.159 | 0.094 | 0.093 |
| | | -0.633 | -1.03 | -0.828 | 0.343 | -0.148 |

Design 1-CE50 with modal suppression

| | | | | | | |
|-------|---|-------|-------|--------|-------|--------|
| G_p | = | -22.8 | 1.91 | -0.658 | -2.16 | 0.856 |
| | | -41.4 | 1.60 | -2.66 | -2.41 | 1.92 |
| | | -42.1 | -5.27 | -2.61 | 5.74 | 0.365 |
| G_v | = | -1.78 | -1.54 | 0.998 | 1.21 | -0.918 |
| | | -8.03 | -1.54 | 0.838 | 1.65 | -0.097 |
| | | 3.49 | 0.011 | 0.147 | 0.434 | 0.313 |

Design 1-MCE50 with modal suppression

$$G_p = \begin{matrix} -18.3 & -0.092 & -1.48 & 4.64 & -1.46 \\ -30.6 & -4.05 & -3.26 & 3.83 & -12.5 \\ -22.5 & -3.67 & -1.58 & -1.46 & -7.66 \end{matrix}$$

$$G_v = \begin{matrix} -0.857 & -3.49 & -3.72 & -1.26 & -8.23 \\ 5.62 & 0.436 & -0.234 & -0.159 & 0.296 \\ 1.08 & -0.124 & -1.36 & 0.256 & -1.49 \end{matrix}$$

Design 2-MCE50 with modal suppression

$$G_p = \begin{matrix} -166 & -3.28 & 1.98 & 2.26 & -2.89 \\ 74.0 & -60.4 & 18.8 & 23.2 & 50.9 \\ 4.62 & 128 & -49.5 & -61.4 & -47.6 \end{matrix}$$

$$G_v = \begin{matrix} -22.1 & -19.4 & 5.50 & 7.15 & 16.9 \\ 14.8 & -27.8 & 10.8 & 14.2 & 13.0 \\ -19.0 & -12.8 & 1.88 & 2.14 & 17.8 \end{matrix}$$

Appendix C: Weighting Matrices

All weighting matrices W_H [in Eq (5-6)] were diagonal matrices. For all but two designs, the matrices were identity matrices.

For design 1-MCE50, the first 12 diagonal elements were 1, 1, 10, 10, 10, 10, 100, 100, 10, 10, 100, 100; the rest were ones - i. e., the elements of W_H corresponding to the actuator locations and two inboard sensor locations on each arm (ρ_{u1} , ρ_{u2} , ρ_{s1} , ρ_{s2} , ρ_{s5} , ρ_{s6}) were 10, and the weights on the two outboard sensors on each arm (ρ_{s3} , ρ_{s4} , ρ_{s7} , ρ_{s8}) were 100.

For design 2-CE50, the first 12 diagonal elements were 1, 1, 0.1, 0.1, 0.1, 0.1, 0.1, 0.1, 0.1, 0.1, 0.1, 0.1; the rest were ones - i.e., the elements of W_H corresponding to the sensor and actuator locations were all 0.1.

Bibliography

1. Weisshaar, T.A., J.R. Newsom, T.A. Zeiler and M.G. Gilbert. "Integrated Structure/Control Design - Present Methodology and Future Opportunities," Proceedings of the 15th Congress of the International Council of the Aeronautical Sciences. 1119-1128. London, September 7-12, 1986.
2. Koski, J. "Multicriterion Optimization in Structural Design," New Directions in Optimum Structural Design, Proceedings of the Second International Symposium on Optimum Structural Design, 11th Office of Naval Research Naval Structural Mechanics Symposium, edited by E. Atrek, R.H. Gallagher, K.M. Ragsdell and O.C. Zienkiewicz. 483-503. University of Arizona, Tucson AZ, October 19-22, 1981. New York: John Wiley & Sons, 1984.
3. Jendo, S., W. Marks and G. Thierauf. "Multicriteria Optimization in Optimum Structural Design," Large-Scale Systems, 9: 141-150 (October 1985).
4. Koski, J. and R. Silvennoinen. "Norm Methods and Partial Weighting in Multicriterion Optimization of Structures," International Journal for Numerical Methods in Engineering, 24: 1101-1121 (June 1987).
5. Koski, J. "Defectiveness of Weighting Methods in Multicriterion Optimization of Structures," Communications in Applied Numerical Methods, 1: 333-337 (1985).
6. Dlesk, D.C. and J.S. Liebman. "Multiple Objective Engineering Design," Engineering Optimization, 6: 161-175 (1983).
7. Chankong, V. and Y.Y. Haimes. Multiobjective Decision Making: Theory and Methodology. New York: Elsevier Science Publishing Company, 1983.
8. Cohon, J.L. Multiobjective Programming and Planning. New York: Academic Press, 1978.
9. Goicoechea, A., D.R. Hansen and L. Duckstein. Multiobjective Decision Analysis with Engineering and Business Applications. New York: John Wiley & Sons, Inc., 1982.
10. Zeleny, M. Multiple Criteria Decision Making. New York: McGraw-Hill Book Company, 1982.
11. Salukvadze, M.E. Vector-Valued Optimization Problems in Control Theory. New York: Academic Press, 1979.
12. Stadler, W. "Multicriteria Optimization in Mechanics (A Survey)," Applied Mechanics Reviews, 37: 277-286 (March 1984).

13. Rao, S.S., V.B. Venkayya and N.S. Khot. "Optimization of Actively Controlled Structures Using Goal Programming Techniques," International Journal for Numerical Methods in Engineering, 26: 183-197 (January 1988).
14. Rao, S.S. "Game Theory Approach for Multiobjective Structural Optimization," Computers & Structures, 25: 119-127 (1987).
15. Carmichael, D.G. "Computation of Pareto Optima in Structural Design," International Journal for Numerical Methods in Engineering, 15: 925-929 (June 1980).
16. Duckstein, L. "Multiobjective Optimization in Structural Design: The Model Choice Problem," New Directions in Optimum Structural Design, Proceedings of the Second International Symposium on Optimum Structural Design, 11th Office of Naval Research Naval Structural Mechanics Symposium, edited by E. Atrek, R.H. Gallagher, K.M. Ragsdell and O.C. Zienkiewicz. 459-481. University of Arizona, Tucson AZ, October 19-22, 1981. New York: John Wiley & Sons, Inc., 1984.
17. Rao, S.S. "Multiobjective Optimization in Structural Design with Uncertain Parameters and Stochastic Processes," AIAA Journal, 22: 1670-1678 (November 1984).
18. Rew, D.W. New Feedback Design Methodologies for Large Space Structures: A Multi-Criterion Optimization Approach. PhD Dissertation. Virginia Polytechnic Institute and State University, Blacksburg VA, 1987.
19. Rew, D.W. and J.L. Junkins. "Multi-criterion Approaches to Optimization of Linear Regulators," The Journal of the Astronautical Sciences, 36: 199-217 (July-September 1988).
20. Junkins, J.L. and D.W. Rew. "Unified Optimization of Structures and Controllers," Large Space Structures : Dynamics and Control, edited by S.N. Atluri and A.K. Amos. 323-353. Berlin: Springer-Verlag, 1988.
21. Bodden, D.S. and J.L. Junkins. "Eigenvalue Optimization Algorithms for Structure/Controller Design Iterations," Journal of Guidance, Control, and Dynamics, 8: 697-706 (November-December 1985).
22. Muckenthaler, T.V. Incorporating Control into the Optimal Structural Design of Large Flexible Space Structures. MS Thesis, AFIT/GA/AA/84D-7. School of Engineering, Air Force Institute of Technology (AU), Wright-Patterson AFB OH, December 1984 (AD-A152858).
23. Rew, D.W. and J.L. Junkins. "In Search of the Optimal Quadratic Regulator," Proceedings of the Fifth VPI&SU/AIAA Symposium on Dynamics and Control of Large Structures. 109-123. Blacksburg VA, June 12-14, 1985.
24. Junkins, J.L. "Equivalence of the Minimum Norm and Gradient Projection Constrained Optimization Techniques," AIAA Journal, 10: 927-929 (July 1972).

25. Sesak, J.R., P.W. Likins and J. Coradetti. "Flexible Spacecraft Control by Model Error Sensitivity Suppression," The Journal of the Astronautical Sciences, 27: 131-156 (April-June 1979).
26. Longman, R.W. "Annihilation or Suppression of Control and Observation Spillover in the Optimal Shape Control of Flexible Spacecraft," The Journal of the Astronautical Sciences, 27: 381-399 (October-December 1979).
27. Calico, R.A. Jr. and W.T. Miller. "Decentralized Control for a Flexible Spacecraft," Proceedings AIAA/AAS Astrodynamics Conference. AIAA-82-1404. San Diego CA, August 9-11, 1982.
28. Calico, R.A. "Decoupled Direct Output Feedback Control of a Large Space Structure," Proceedings of SECTAM XII - The Southeastern Conference on Theoretical and Applied Mechanics. 309-313. Callaway Gardens GA, May 10-11, 1984.
29. Calico, R.A. and F.E. Eastep. "Structural Design and Decoupled Control," Acta Astronautica, 19: 9-15 (January 1989).

Vita

Captain Garret L. Schneider [REDACTED] 1952 in [REDACTED] Washington. He received his Bachelor of Science in Aeronautics and Astronautics in 1980 from the University of Washington (Seattle, Washington) and was commissioned in the U.S. Air Force following Officer Training School. He served as a flight test and simulation engineer at the Air Force Flight Test Center, Edwards AFB, California until May, 1983. He then attended the Air Force Institute of Technology (AFIT) School of Engineering in residence at Wright-Patterson AFB, Ohio, receiving a Master of Science in Aeronautical Engineering in December, 1984. Captain Schneider was then assigned to Headquarters, AF Space Division, Los Angeles AFS, California, where he managed space systems survivability programs for the Strategic Defense Initiative until returning to AFIT (School of Engineering) in June, 1987 to begin the resident doctoral program.

[REDACTED]

[REDACTED] 4

REPORT DOCUMENTATION PAGE

Form Approved
OMB No. 0704-0188

| | | | | | |
|---|-------|--|---|--|-------------------------------|
| 1a. REPORT SECURITY CLASSIFICATION UNCLASSIFIED | | | 1b. RESTRICTIVE MARKINGS | | |
| 2a. SECURITY CLASSIFICATION AUTHORITY | | | 3. DISTRIBUTION / AVAILABILITY OF REPORT | | |
| 2b. DECLASSIFICATION / DOWNGRADING SCHEDULE | | | Approved for public release; distribution unlimited | | |
| 4. PERFORMING ORGANIZATION REPORT NUMBER(S) AFIT/DS/ENY/90-02 | | | 5. MONITORING ORGANIZATION REPORT NUMBER(S) | | |
| 6a. NAME OF PERFORMING ORGANIZATION School of Engineering | | 6b. OFFICE SYMBOL (If applicable) AFIT/ENY | 7a. NAME OF MONITORING ORGANIZATION | | |
| 6c. ADDRESS (City, State, and ZIP Code) Air Force Institute of Technology (AU) Wright-Patterson AFB, Ohio 45433-6583 | | | 7b. ADDRESS (City, State, and ZIP Code) | | |
| 8a. NAME OF FUNDING / SPONSORING ORGANIZATION | | 8b. OFFICE SYMBOL (If applicable) | 9. PROCUREMENT INSTRUMENT IDENTIFICATION NUMBER | | |
| 8c. ADDRESS (City, State, and ZIP Code) | | | 10. SOURCE OF FUNDING NUMBERS | | |
| | | | PROGRAM ELEMENT NO. | PROJECT NO. | TASK NO. |
| | | | WORK UNIT ACCESSION NO. | | |
| 11. TITLE (Include Security Classification) INTEGRATED STRUCTURAL/CONTROL DESIGN VIA MULTIOBJECTIVE OPTIMIZATION | | | | | |
| 12. PERSONAL AUTHOR(S) Garret L. Schneider, B.S., M.S., Captain, USAF | | | | | |
| 13a. TYPE OF REPORT PhD Dissertation | | 13b. TIME COVERED FROM _____ TO _____ | | 14. DATE OF REPORT (Year, Month, Day) 1990, May | |
| 15. PAGE COUNT 87 | | | | | |
| 16. SUPPLEMENTARY NOTATION | | | | | |
| 17. COSATI CODES | | | 18. SUBJECT TERMS (Continue on reverse if necessary and identify by block number) | | |
| FIELD | GROUP | SUB-GROUP | | | |
| 12 | 02 | | Optimization, Control Theory, Flexible Structures, | | |
| 22 | 02 | | Combinatorial Analysis, Mathematical Analysis | | |
| 19. ABSTRACT (Continue on reverse if necessary and identify by block number) | | | | | |
| Research Committee Chairman: Dr Robert A. Calico, Jr. Interim Dean, School of Engineering | | | | | |
| 20. DISTRIBUTION / AVAILABILITY OF ABSTRACT <input checked="" type="checkbox"/> UNCLASSIFIED/UNLIMITED <input type="checkbox"/> SAME AS RPT. <input type="checkbox"/> DTIC USERS | | | 21. ABSTRACT SECURITY CLASSIFICATION UNCLASSIFIED | | |
| 22a. NAME OF RESPONSIBLE INDIVIDUAL Robert A. Calico, Jr. Interim Dean | | | 22b. TELEPHONE (Include Area Code) (513) 255-3025 | | 22c. OFFICE SYMBOL AFIT/EN |

Block 19:

A minimum correction homotopy approach is used to obtain the simultaneous/integrated optimal design of a large flexible structure and its active control system. Instead of the usual method of weighting and summing all desired objectives to form a constrained scalar optimization problem, a vector of objective functions is dealt with directly. The Draper/RPL configuration (a central hub with four symmetric, identical arms) is the design structure. The design seeks to minimize the mass of the arms. Using simple feedback of arm displacements and velocities, the control system seeks to achieve specified closed-loop eigenvalues (frequencies and damping ratios) and control effort. Design variables are the arm dimensions, control system gains, and sensor and actuator locations. Not only can the structural design be accomplished while placing the closed-loop eigenvalues, but a simultaneous 50% reduction in mass and/or control effort can be obtained. Since reduced-order models were used for the structural/control design, the resultant configurations are easily driven unstable by spillover from higher-order unmodeled modes. A modal suppression technique is applied to eliminate observation spillover and provide a decade of deadband above the controller bandwidth.